Chapter 4
Representations

Abstract Having made acquaintance with the basic properties of groups, we now turn our attention to the structure of the matrices that represent the group action in a function space. It turns out that there exists only a limited set of standard patterns. These are called the irreducible representations. They form the principal mathematical concept on which this monograph is based, and much care is devoted to acquire a gradual understanding of what this concept really means. Then the character theorem, matrix theorems, and projection operators are introduced. The concepts of subduction and induction relate the representations of subgroups and those of their parent groups. The chapter also offers a detailed group-theoretical analysis of three chemical applications: the tetrahedral hybridization of carbon, the molecular vibrations of UF_6, and the electronic structure of conjugated hydrocarbons, according to the Hückel model and the method of the London model of gauge-invariant atomic orbitals.

Contents

A.J. Ceulemans, *Group Theory Applied to Chemistry*, Theoretical Chemistry and Computational Modelling, DOI 10.1007/978-94-007-6863-5_4,

4.1 Symmetry-Adapted Linear Combinations of Hydrogen Orbitals in Ammonia

From now on we shall no longer be working with the nuclei, but with electronic orbital functions that are anchored on the nuclei. As an example, we take the $1s$ orbitals on the hydrogen atoms in ammonia. The $|1s_\mathrm{A}\rangle$ is defined in Eq. (4.1), where $\mathbf{R}_\mathrm{A}$ denotes the position vector of atom A with respect to the Cartesian origin; a_0 is the Bohr radius (0.529 Å), which is the atomic unit of length.

$$|1s_\mathrm{A}\rangle = \frac{1}{\sqrt{\pi}}\left(\frac{1}{a_0}\right)^{3/2} \exp\left(-\frac{|\mathbf{r}-\mathbf{R}_\mathrm{A}|}{a_0}\right) \tag{4.1}$$

Following Sect. 1.2, the transformation of this function by the threefold axis is given by

$$\hat{C}_3|1s_\mathrm{A}\rangle = \frac{1}{\sqrt{\pi}}\left(\frac{1}{a_0}\right)^{3/2} \exp\left(-\frac{|[\hat{C}_3^{-1}\mathbf{r}]-\mathbf{R}_\mathrm{A}|}{a_0}\right) \tag{4.2}$$

The distance between the electron at position $\hat{C}_3^{-1}\mathbf{r}$ and nucleus A is equal to the distance between the electron at position $\mathbf{r}$ and nucleus B. This can be established by working out the distances as functions of the Cartesian coordinates, but a straightforward demonstration is based on the fact that the distance does not change if we rotate *both* nuclei and electrons:

$$\left|\left[\hat{C}_3^{-1}\mathbf{r}\right]-\mathbf{R}_\mathrm{A}\right| = \hat{\mathcal{Q}}_3\left|\left[\hat{C}_3^{-1}\mathbf{r}\right]-\mathbf{R}_\mathrm{A}\right| = \left|\left[\hat{\mathcal{Q}}_3\hat{C}_3^{-1}\mathbf{r}\right]-\hat{\mathcal{Q}}_3\mathbf{R}_\mathrm{A}\right| = |\mathbf{r}-\mathbf{R}_\mathrm{B}| \tag{4.3}$$

Here, we have denoted the bodily rotation of the entire molecule as $\hat{\mathcal{Q}}_3$ in order to indicate that its action also involves the nuclei, as opposed to $\hat{C}_3$, which is reserved for electrons. In the expression of Eq. (4.1), $\mathbf{R}_\mathrm{A}$ is replaced by $\mathbf{R}_\mathrm{B}$, or

$$\hat{C}_3|1s_\mathrm{A}\rangle = |1s_\mathrm{B}\rangle \tag{4.4}$$

This confirms the active view, propagated from the beginning, as applied to the functions. We rotate the $|1s_\mathrm{A}\rangle$ orbital itself counterclockwise over 120°. The result is equal to the $|1s_\mathrm{B}\rangle$ orbital. We now put the three components of the function space together in a row vector:

$$|\mathbf{f}\rangle = \begin{pmatrix} |1s_\mathrm{A}\rangle & |1s_\mathrm{B}\rangle & |1s_\mathrm{C}\rangle \end{pmatrix} \tag{4.5}$$

The action of the operator in the function space now reads as follows:

$$\hat{C}_3|\mathbf{f}\rangle = |\mathbf{f}\rangle\mathbb{D}(C_3) \tag{4.6}$$

where the representation matrix is given by

$$\mathbb{D}(C_3) = \begin{pmatrix} 0 & 0 & 1 \\ 1 & 0 & 0 \\ 0 & 1 & 0 \end{pmatrix} \tag{4.7}$$

While the function space is clearly invariant, i.e., it transforms into itself under the rotation, the individual components are not: they are mutually permuted. Our objective is to find *symmetry-adapted linear combinations* (SALCs) that are invariant under the operator, except, possibly, for a phase factor. The combinations we are looking for are thus nothing other than eigenfunctions of the symmetry operator, in the same way as solutions of the Schrödinger equation are eigenfunctions of the Hamiltonian. Unlike the Hamiltonian eigenfunctions, however, which will usually consist of linear combinations in an infinite Hilbert space, the present exercise is carried out in a space of three functions only since this space is already closed under the operator. We shall solve this symmetry eigenvalue problem in a purely algebraic way. Let $|\psi_m\rangle$ be a SALC:

$$|\psi_m\rangle = \sum_{\mathrm{X=A,B,C}} c_{\mathrm{X}} |1s_{\mathrm{X}}\rangle \tag{4.8}$$

which we shall again write as the product of a row vector and a column vector:

$$|\psi_m\rangle = \begin{pmatrix} |1s_{\mathrm{A}}\rangle & |1s_{\mathrm{B}}\rangle & |1s_{\mathrm{C}}\rangle \end{pmatrix} \begin{pmatrix} c_{\mathrm{A}} \\ c_{\mathrm{B}} \\ c_{\mathrm{C}} \end{pmatrix} \tag{4.9}$$

The transformation of this function is then given by

$$\hat{C}_3 |\psi_m\rangle = |\mathbf{f}\rangle \begin{pmatrix} 0 & 0 & 1 \\ 1 & 0 & 0 \\ 0 & 1 & 0 \end{pmatrix} \begin{pmatrix} c_{\mathrm{A}} \\ c_{\mathrm{B}} \\ c_{\mathrm{C}} \end{pmatrix} \tag{4.10}$$

We now require this function to be an eigenfunction of the threefold rotation operator with eigenvalue λ:

$$\hat{C}_3 |\psi_m\rangle = \lambda |\psi_m\rangle \tag{4.11}$$

Combining Eqs. (4.10) and (4.11), we see that the function is an eigenfunction if the product of the $\mathbb{D}$ matrix with the column vector of the coefficients returns the coefficient column, multiplied by the eigenvalue λ, i.e.,

$$\begin{pmatrix} 0 & 0 & 1 \\ 1 & 0 & 0 \\ 0 & 1 & 0 \end{pmatrix} \begin{pmatrix} c_{\mathrm{A}} \\ c_{\mathrm{B}} \\ c_{\mathrm{C}} \end{pmatrix} = \lambda \begin{pmatrix} c_{\mathrm{A}} \\ c_{\mathrm{B}} \\ c_{\mathrm{C}} \end{pmatrix} \tag{4.12}$$

This equation can also be rewritten as

$$\begin{pmatrix} -\lambda & 0 & 1 \\ 1 & -\lambda & 0 \\ 0 & 1 & -\lambda \end{pmatrix} \begin{pmatrix} c_{\mathrm{A}} \\ c_{\mathrm{B}} \\ c_{\mathrm{C}} \end{pmatrix} = \mathbf{0} \tag{4.13}$$

Equation (4.13) forms a homogeneous system of equations in the three unknowns. It will have solutions only if the matrix preceding the column vector of the unknowns

has determinant zero. This requirement is written as

$$\left|\mathbb{D}(C_3) - \lambda\mathbb{I}\right| = 0 \tag{4.14}$$

Here, the vertical bars denote the determinant. Equation (4.14) is called the *secular equation*. It has the form of a simple cubic equation in the eigenvalue λ:

$$-\lambda^3 + 1 = 0 \tag{4.15}$$

This equation is the Euler equation. It has three roots:

$$\lambda_m = \exp\left(\frac{2m\pi i}{3}\right) \tag{4.16}$$

where m can take the values $-1, 0, +1$. What we have just performed is a matrix diagonalization of the representation matrix. We obtain at once not one but three eigenvalues. The eigenfunction corresponding to a given root can now be found by introducing this λ value in the system of equations, Eq. (4.13). Since the system is homogeneous, the three unknown coefficients can be determined only up to a constant factor. We find the absolute values of these vector coefficients by invoking a normalization condition that requires the vectors to be of unit length. The simplified normalization condition, neglecting overlap integrals, reads:

$$|c_\mathrm{A}|^2 + |c_\mathrm{B}|^2 + |c_\mathrm{C}|^2 = 1 \tag{4.17}$$

In this way we obtain three SALCs, each characterized by a different eigenvalue for the symmetry operator:

$$\begin{aligned}
|\psi_0\rangle &= \frac{1}{\sqrt{3}}\left(|1s_\mathrm{A}\rangle + |1s_\mathrm{B}\rangle + |1s_\mathrm{C}\rangle\right) \\
|\psi_{+1}\rangle &= \frac{1}{\sqrt{3}}\left(|1s_\mathrm{A}\rangle + \bar{\epsilon}|1s_\mathrm{B}\rangle + \epsilon|1s_\mathrm{C}\rangle\right) \\
|\psi_{-1}\rangle &= \frac{1}{\sqrt{3}}\left(|1s_\mathrm{A}\rangle + \epsilon|1s_\mathrm{B}\rangle + \bar{\epsilon}|1s_\mathrm{C}\rangle\right)
\end{aligned} \tag{4.18}$$

where $\epsilon = \exp 2\pi i/3$. The set of corresponding eigenvalues is called the spectrum of the operator. It will be evident that this spectrum consists of the cube roots of 1, since operating with $\hat{C}_3$ three times in succession is equivalent to applying the identity operator:

$$\hat{C}_3^3|\psi_m\rangle = \lambda^3|\psi_m\rangle = \hat{E}|\psi_m\rangle \tag{4.19}$$

For any operator, one can find eigenfunctions by simply diagonalizing the corresponding representation matrix. However, our objective is more ambitious. We want to obtain functions that are not only adapted to a single symmetry element but to the group as a whole. This really amounts to finding SALCs for the set of group generators, since adaptation to the generators implies that the function is adapted to any

combination of generators and, hence, to the whole group. So, in the case of C_{3v}, we have to examine the behavior of the $|\psi_m\rangle$ functions under a vertical symmetry plane as well, say $\hat{\sigma}_1$. This plane will leave $|1s_A\rangle$ unchanged and will interchange $|1s_B\rangle$ and $|1s_C\rangle$. Its effect on the trigonal eigenfunctions is thus given by

$$\begin{aligned}\hat{\sigma}_1|\psi_0\rangle &= |\psi_0\rangle \\ \hat{\sigma}_1|\psi_{+1}\rangle &= |\psi_{-1}\rangle \\ \hat{\sigma}_1|\psi_{-1}\rangle &= |\psi_{+1}\rangle\end{aligned} \tag{4.20}$$

What does this result tell us? The SALC $|\psi_0\rangle$ is simultaneously an eigenfunction of both $\hat{C}_3$ and $\hat{\sigma}_1$; hence, it forms in itself a one-dimensional function space that is completely adapted to the full group. This symmetry characteristic will be denoted by the totally symmetric representation A_1. However, the other two SALCs are transformed into each other. We can easily turn them into eigenfunctions of $\hat{\sigma}_1$ and in this way obtain alternative eigenfunctions, one of which is symmetric under reflection and one of which is antisymmetric. These will be labeled as x and y, respectively, since their symmetry under reflection mimics the symmetries of p_x and p_y:

$$\begin{aligned}|\psi_x\rangle &= \frac{1}{\sqrt{2}}\big(|\psi_{+1}\rangle + |\psi_{-1}\rangle\big) = \frac{1}{\sqrt{6}}\big(2|1s_A\rangle - |1s_B\rangle - |1s_C\rangle\big) \\ |\psi_y\rangle &= \frac{i}{\sqrt{2}}\big(|\psi_{+1}\rangle - |\psi_{-1}\rangle\big) = \frac{1}{\sqrt{2}}\big(|1s_B\rangle - |1s_C\rangle\big)\end{aligned} \tag{4.21}$$

A schematic drawing of these eigenfunctions is shown in Fig. 4.1. The downside of this symmetry adaptation is that it has destroyed the diagonalization along the trigonal axis. Indeed, one has:

$$\hat{C}_3\begin{pmatrix}|\psi_x\rangle & |\psi_y\rangle\end{pmatrix} = \begin{pmatrix}|\psi_x\rangle & |\psi_y\rangle\end{pmatrix}\begin{pmatrix}\cos(2\pi/3) & -\sin(2\pi/3) \\ \sin(2\pi/3) & \cos(2\pi/3)\end{pmatrix} \tag{4.22}$$

Hence, it is impossible to resolve the function space formed by $|\psi_{\pm 1}\rangle$ into simultaneous eigenfunctions of both generators. The action of the symmetry group ties these functions together into a two-dimensional space, which is thus *irreducible*. This symmetry characteristic is denoted by the degenerate irreducible representation E. We have learned form this simple example the following. The construction of SALCs of a symmetry group is based on simultaneous diagonalization of the representation matrices of the group generators. This will resolve the function space into separate blocks, which may consist of one function, or which may form a subspace that cannot be further reduced. The results are functions that transform as irreducible representations (irreps). Why is such a resolution important? The irreducible subspaces into which the function space has been separated are invariant under the actions of the actual symmetry group. This means that there are no operators that send SALCs from one irreducible subspace into SALCs from another irreducible subspace. This also implies that the eigenenergies associated with these

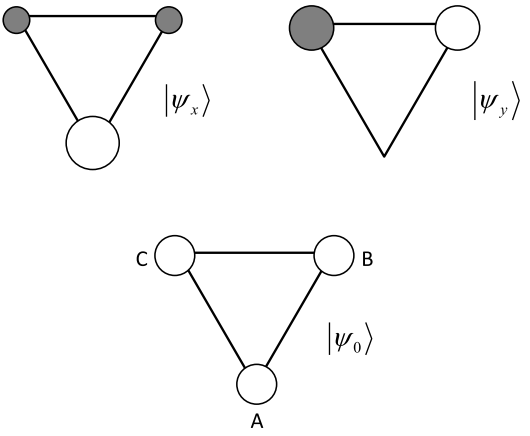

Fig. 4.1 Hydrogen SALCs in ammonia. The size of the circles is proportional to the eigenfunction coefficients. $|\psi_0\rangle$ transforms as the totally symmetric irrep A_1; $|\psi_x\rangle$ and $|\psi_y\rangle$ are components of the degenerate E representation

irreducible blocks are not be related. We will return to this in much more detail in Sect. 5.2. The algebraic treatment also provides an insight into the meaning of degeneracy. The two components of the E irrep are locked in the same function space because it is not possible to diagonalize the representation matrices for both generators simultaneously. If two operators commute, it is always possible to find solutions that are simultaneous eigenfunctions of both. However, the two generators of C_{3v} do not commute as this group is not abelian. The fact that the corresponding representation matrices also do not commute explains why it is impossible to block-diagonalize the E irrep.

4.2 Character Theorems

When examining a function space from a symmetry point of view, we note that there are two basic questions to be asked:

1. What are the symmetry ingredients of the function space; in other words, which irreps describe the symmetry of this space?
2. What do the corresponding SALCs look like?

The present section on characters deals with the first question and provides an elegant description of the symmetries of function spaces. In the subsequent sections, matrix theorems are used for the construction of projection operators that will carry out the job of obtaining the suitable SALCs. The intuitive algebraic approach that we have demonstrated in the previous section has been formalized by Schur, Frobenius,[1] and others into a fully fledged character theory, which reveals which irreps

[1]The papers by Schur and Frobenius have been edited as C. Frobenius, The Collected Works of Frobenius (1849–1917), J.-P. Serre (ed.), Springer, Berlin (1968), 3 vols.; I. Schur, Gesammelte Abhandlungen, A. Brauer and H. Rohrbach (eds.) Springer, Berlin (1973), 3 vols.

a given group can sustain and how to analyze the irreducible contents of a given function space. Characters are nothing other than the traces (that is, the sum of the diagonal elements) of representation matrices. They will be represented as $\chi(R)$:

$$\chi(R) = \sum_i D_{ii}(R) \tag{4.23}$$

If the functional basis of a representation is transformed by a unitary transformation, the trace does not change, as can easily be demonstrated. Define $|\mathbf{f}'\rangle = |\mathbf{f}\rangle\mathbb{U}$. Then the corresponding representation matrices, $\mathbb{D}'(R)$, also undergo a unitary transformation:

$$\begin{aligned}\hat{R}|\mathbf{f}'\rangle &= \hat{R}|\mathbf{f}\rangle\mathbb{U} = |\mathbf{f}\rangle\mathbb{D}(R)\mathbb{U} \\ &= |\mathbf{f}'\rangle\mathbb{U}^{-1}\mathbb{D}(R)\mathbb{U} \\ &= |\mathbf{f}'\rangle\mathbb{D}'(R)\end{aligned} \tag{4.24}$$

from which it follows that

$$\mathbb{D}'(R) = \mathbb{U}^{-1}\mathbb{D}(R)\mathbb{U} \tag{4.25}$$

or, for unitary $\mathbb{U}$, that

$$\begin{aligned}D'_{ij}(R) &= \sum_{kl} \bar{U}^T_{ik} D_{kl}(R) U_{lj} \\ &= \sum_{kl} \bar{U}_{ki} D_{kl}(R) U_{lj}\end{aligned} \tag{4.26}$$

The invariance of the character then follows from the orthogonality of the rows of the unitary matrix:

$$\begin{aligned}\chi'(R) &= \sum_i D'_{ii}(R) \\ &= \sum_{kl} D_{kl}\left(\sum_i \bar{U}_{ki} U_{li}\right) \\ &= \sum_{kl} D_{kl}(R)\delta_{kl} \\ &= \sum_k D_{kk}(R) \\ &= \chi(R)\end{aligned} \tag{4.27}$$

Hence, sets of characters literally characterize representations since they are immune to the effects of unitary transformations, such as occur in Eq. (4.21) between the complex functions $|\psi_{+1}\rangle, |\psi_{-1}\rangle$ and the real functions $|\psi_x\rangle, |\psi_y\rangle$. The characters for the irreps are brought together in a character table. Here, the conjugacy class

Table 4.1 Character table for the group C_{3v} and reducible characters of the hydrogen $1s$ functions $\chi(1s)$ and hydrogen bends $\chi(\Delta\phi)$. The $\chi(1s)$ row is equal to the sum of the A_1 and E rows, and the $\chi(\Delta\phi)$ row is equal to the sum of the A_2 and E rows

C_{3v}	$\hat{E}$	$2\hat{C}_3$	$3\hat{\sigma}_v$	$\langle\chi\|\chi\rangle$
A_1	1	1	1	6
A_2	1	1	−1	6
E	2	−1	0	6
$\chi(1s)$	3	0	1	12
$\chi(\Delta\phi)$	3	0	−1	12

concept comes in very useful. Indeed, since all elements belonging to the same class are similarity transforms, their representation matrices are unitary transforms and, hence, all have the same character. We can thus group elements together in classes. In Table 4.1 we show the character table for C_{3v} as can be obtained by algebraic techniques such as the one we used in the previous section. We recognize at once the characters for the totally symmetric A_1 and the twofold-degenerate E irrep. In addition, there is another one-dimensional irrep, A_2, which is symmetric under the threefold axis and antisymmetric under the reflection planes.

Let us denote an irrep as Γ_i and the string of characters, arranged in a row over the full group, in a Dirac form as $|\chi^{\Gamma_i}\rangle$. The norm of this string[2] will then be denoted as a bracket, i.e.,

$$\langle\chi^{\Gamma_i}|\chi^{\Gamma_i}\rangle = \sum_{R\in G} \bar{\chi}^{\Gamma_i}(R)\chi^{\Gamma_i}(R) \tag{4.28}$$

Since the matrices are unitary, we could also replace the complex-conjugate character by the character of the inverse element:

$$\bar{\chi}^{\Gamma_i}(R) = \chi^{\Gamma_i}\left(R^{-1}\right) \tag{4.29}$$

The character strings obey the following character theorem:

Theorem 4 *The norm of the character string is equal to the order of the group if and only if the characters refer to an irreducible representation. The scalar product of two character strings of different irreps is equal to zero.*

This theorem can be expressed as follows:

$$\langle\chi^{\Gamma_i}|\chi^{\Gamma_j}\rangle = \sum_{R\in G} \bar{\chi}^{\Gamma_i}(R)\chi^{\Gamma_j}(R) = \delta_{ij}|G| \tag{4.30}$$

where Γ_i and Γ_j refer to irreducible representations, and $|G|$ is the order of the group. This theorem provides an elegant and simple solution for determining the ir-

[2]Since elements in the same class have the same character, we can also simplify the expression to a summation over all classes, provided that we then multiply each term by the number of elements in the class under consideration.

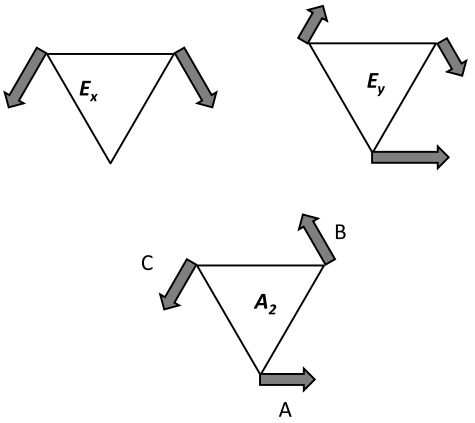

Fig. 4.2 Symmetry coordinates for the in-plane bending of the hydrogen atoms in ammonia. The length of *the arrows* is proportional to the SALC coefficients

rep content of a function space. One first determines the characters of the representation matrices, $\chi(R)$. They will be equal to the sums of the traces of the individual irreducible symmetry blocks. This can be expressed as follows:

$$\chi(R) = \sum_i c_i \chi^{\Gamma_i}(R) \tag{4.31}$$

Here, the important quantities are the c_i coefficients. These are integers that tell how many times a given irrep Γ_i is contained in the function space. They can easily be calculated by using the character theorems. All one has to do is to evaluate the scalar product of a given irreducible character, say Γ_k, and the reducible character, and then divide by the group order.

$$\frac{1}{|G|}\langle \chi^{\Gamma_k} | \chi \rangle = \frac{1}{|G|} \sum_i c_i \langle \chi^{\Gamma_k} | \chi^{\Gamma_i} \rangle = \sum_i c_i \delta_{ki} = c_k \tag{4.32}$$

It is also clear that the norm of the reducible character is a multiple of the group order, since

$$\langle \chi | \chi \rangle = \sum_{ij} c_i c_j \langle \chi^{\Gamma_i} | \chi^{\Gamma_j} \rangle = \sum_i c_i^2 |G| \tag{4.33}$$

This procedure may seem quite complicated, but it is in fact very simple. Let us demonstrate this for the previous example, the set of the three $1s$-orbitals on the hydrogens in NH_3. We first determine the reducible character of this set (see $\chi(1s)$ in Table 4.1). We do not have to do this for all six elements of C_{3v} but only for one representative of each class since conjugate elements have the same characters. For the unit element, the representation matrix is of course the 3×3 unit matrix, and its trace is equal to three, the dimension of the set. For the other elements, we do not need to know the full matrix representation; indeed, *we need only the elements on the diagonal.* Now a diagonal entry in a representation matrix can differ from zero only if a component function is turned into itself, or at least into a fraction of itself.

The threefold axis moves all three $1s$-orbitals around and hence has zeros only on the diagonal; thus, $\chi(C_3) = 0$ (see Eq. (4.7)). For the reflection planes, one element is stabilized, while the other two are interchanged; hence, there is only one nonzero diagonal element, which will be equal to $+1$ since the orbital is not affected; hence, $\chi(\sigma_1) = +1$. The norm of the character string is given by

$$\langle \chi | \chi \rangle = 3^2 + 2 \times 0 + 3 \times 1^2 = 12 = 2|C_{3v}| \tag{4.34}$$

Since the norm is twice the order of the group, we know for certain that the symmetry of the function space is reducible. In fact, we also predict that it will reduce to two irreps, each of which occurs once, since the sum of the squares of the multiplicities in Eq. (4.33) is equal to 2. These coefficients can now be obtained by calculating the character brackets, which yields the previous result: $c_{A_1} = 1, c_{A_2} = 0, c_E = 1$. From Table 4.1 one can also verify that the sum of χ^{A_1} and χ^{E} equals $\chi(1s)$. This is sometimes also expressed in a formal way as

$$\Gamma = A_1 + E \tag{4.35}$$

As a further example, we can take the set of the two in-plane $2p$-orbitals on nitrogen, p_x and p_y. Here, the character for the threefold axis is

$$\chi^{p_x, p_y}(C_3) = 2\cos(2\pi i/3) = -1 \tag{4.36}$$

Under the $\hat{\sigma}_1$ plane of symmetry, one of the orbitals is antisymmetric, while the other is symmetric, and so the trace of the matrix vanishes. The characters of this p-set are thus precisely the ones for the E irrep, and we can therefore state that the set $\{p_x, p_y\}$ transforms irreducibly as the E representation. As a final example, let us take the alternative set consisting of three counterclockwise displacement vectors of the hydrogen atoms, along a tangent to the (imagined) circumscribed circle through the hydrogens, as indicated in Fig. 4.2. In this example the function space is the set of three bendings: $\Delta\phi_\mathrm{A}, \Delta\phi_\mathrm{B}, \Delta\phi_\mathrm{C}$. We must realize that in this case the function on which we are operating is actually the distortion itself, and to rotate this distortion in an active sense means to take the distortion vector and displace it to the next nucleus. Hence, nuclei are left immobile: only the distortions are moved. One could easily reconcile this view with the previous orbital rotations by thinking of the distortions as little tangent p-orbitals with positive and negative lobes corresponding to the head and tail of the vectors, respectively. Hence, as an example, one has

$$\hat{C}_3 \Delta\phi_\mathrm{A} = \Delta\phi_\mathrm{B} \tag{4.37}$$

Since all distortions are cyclically permuted, the character under this generator is zero. On the other hand, for the reflection plane, one has:

$$\begin{aligned} \hat{\sigma}_1 \Delta\phi_\mathrm{A} &= -\Delta\phi_\mathrm{A} \\ \hat{\sigma}_1 \Delta\phi_\mathrm{B} &= -\Delta\phi_\mathrm{C} \\ \hat{\sigma}_1 \Delta\phi_\mathrm{C} &= -\Delta\phi_\mathrm{B} \end{aligned} \tag{4.38}$$

In this case, the only contribution to the trace comes from the distortion of A, which is mapped onto minus itself; hence, $\chi(\sigma_1) = -1$. The resulting character string also has norm 12, but in this case it decomposes into $A_2 + E$. As shown in Fig. 4.2, the A_2 component is the sum of the three distortions, which corresponds to a bodily rotation of the molecule around its vertical axis. The E components are given by

$$\begin{aligned} Q_{E_x} &= \frac{1}{\sqrt{2}}(\Delta\phi_{\mathrm{C}} - \Delta\phi_{\mathrm{B}}) \\ Q_{E_y} &= \frac{1}{\sqrt{6}}(2\Delta\phi_{\mathrm{A}} - \Delta\phi_{\mathrm{B}} - \Delta\phi_{\mathrm{C}}) \end{aligned} \tag{4.39}$$

Perhaps the most surprising result is that the symmetry eigenfunctions of the C_{3v} group can be only of three different types: A_1, A_2, and E. In fact, this is another result derived by Schur.

Theorem 5 *The number of irreps in a group is equal to the number of conjugacy classes.*

The fact that there are only a few canonical ways of representing a symmetry group can be rationalized in a general way as follows. Consider a molecule with symmetry group G and a function that is localized on an arbitrary point in the molecule, i.e., a point which is lying neither on an axis of symmetry, nor in a reflection plane, nor in the inversion center or the center of a rotation–reflection axis. We shall denote this function as $|f_E\rangle$ since it is stabilized by, and only by, the unit element. Any other element would move this function to some other point that is a copy of the original one. We write this as

$$\hat{R}|f_E\rangle = |f_R\rangle \tag{4.40}$$

In this way the entire group generates a set of $|G|$ functions, which all are different. Indeed, suppose that, for $\hat{R} \neq \hat{S}$, the two corresponding functions are the same; then the product operation $\hat{S}^{-1}\hat{R}$ maps $|f_E\rangle$ onto itself. This contradicts the assumption that $|f_E\rangle$ is stabilized only by the unit element. Furthermore, the closure of the group also guarantees that this set of functions forms an invariant function space. This function space transforms according to a reducible representation, which is called the *regular* representation, Γ_{reg}. This representation describes the most general function basis that one can consider since it is based on functions that have no symmetry whatsoever. Now let us determine the symmetry ingredients of this space using the standard character procedure. The character of the regular representation is equal to $|G|$ for the unit element and zero for all other elements since none of the functions is stabilized:

$$\chi^{\Gamma_{reg}}(R) = |G|\delta_{ER} \tag{4.41}$$

Inserting this result into the expression for the multiplicity coefficients yields

$$c_k = \frac{1}{|G|}\langle \chi^{\Gamma_k} | \chi^{\Gamma_{reg}} \rangle = \bar{\chi}^{\Gamma_k}(E) = \dim(\Gamma_k) \tag{4.42}$$

Hence, every irrep occurs as many times as its own dimension. The sum of all these irreducible blocks must yield the regular representation. Thus one has

$$\sum_k c_k \dim(\Gamma_k) = \sum_k \left[\dim(\Gamma_k)\right]^2 = |G| \tag{4.43}$$

This result tells us that, in a group of order $|G|$, there are exactly $|G|$ independent vectors. Rewriting these vectors in the form of SALCs exhausts all possible symmetries that can be realized in this group. If a group is abelian, every class is a singleton, and hence the number of classes is equal to the order of the group. In this case, Eq. (4.43) can be fulfilled only if all irreps are one-dimensional. Hence, in an abelian group all irreps are one-dimensional.

4.3 Character Tables

In Appendix A, we reproduce the character tables for the point groups and the symmetric groups, following the standard form introduced by Mulliken [1]. The top row of the table lists the conjugacy classes. In some cases the designations of the symmetry operations can be ambiguous, and additional labels are added, such as h, v, and d for *horizontal*, *vertical*, and *dihedral*, respectively (see also, e.g., Fig. 3.10). In the final columns of the tables we list some simple functions, which transform according to the corresponding irreps. Irreps are denoted by letters that are related to their degeneracy. A and B stand for one-dimensional irreps, which are symmetric or antisymmetric with respect to some principal symmetry element. E and T are used for two- and three-dimensional irreps, respectively. Sometimes, in physics textbooks, T is replaced by F. This alphabetical order is then continued for the fourfold- and fivefold-degenerate irreps in the icosahedral symmetry, which are denoted as G and H. Further subscripts are added to distinguish symmetry characteristics with respect to secondary symmetry elements. Best known are the g and u subscripts, which distinguish between even (*gerade*) and odd (*ungerade*) symmetries with respect to spatial inversion. Primes or double primes are used to distinguish symmetric versus antisymmetric behavior with respect to a horizontal symmetry plane in groups such as $D_{(2n+1)h}$ or $C_{(2n+1)h}$. In addition, numerical indices can appear as subscripts, such as in A_1, A_2 in the C_{3v} group. It should be clear that this labeling is somewhat ad hoc, and one should consult the actual tables in order to find out the precise meaning of the symbols used.

Some point groups, viz. the cyclic groups C_n, $C_{(2n+1)h}$, S_{2n}, and also T and T_h, have irreps with complex characters. In these cases, for an irrep Γ_k with complex characters, there will always be a complementary irrep with a complex-conjugate character string, which is denoted as $\bar{\Gamma}_k$. Hence, one has

$$\chi^{\bar{\Gamma}_k}(R) = \bar{\chi}^{\Gamma_k}(R) \tag{4.44}$$

Note that if Γ_k fulfills the character theorems, then $\bar{\Gamma}_k$ also does, and hence it, too, must be irreducible. The two irreps are said to be complex conjugates. They are orthogonal to each other, and hence there is no point group operation that can turn a function belonging to Γ_k into a function belonging to $\bar{\Gamma}_k$. For this reason, we also should denote them by two separate labels. However, in the absence of external magnetic fields, symmetry is not restricted to spatial symmetry, but also includes time-reversal symmetry. As we have seen in Sect. 2.4, this symmetry will precisely turn functions into their complex conjugates and thus also interchange the corresponding conjugate irreps. Complex-conjugate irreps thus remain degenerate under time reversal, and for this reason, they are usually indicated by means of a brace.

4.4 Matrix Theorem

Determining the symmetry contents of a function space is only a first step. We would also like to know what are the SALCs that correspond to the different irreps. To carry out this task, we have to work with the representation matrices themselves. In the group C_{3v} the matrices for the one-dimensional irreps A_1 and A_2 are trivial since these are simply equal to the corresponding characters. For the E irrep, we need to determine the generator matrices and perform the proper multiplications in order to generate all $\mathbb{D}^E(R)$ for the whole group. These matrices are already available from Table 3.2 for the standard basis of the p_x and p_y orbitals. An important theorem, known as the *Great Orthogonality Theorem* (GOT), is due to Schur.

Theorem 6 *Let Ω and Ω' be two irreducible representations of a group G, and consider vectors formed by taking elements $\{ij\}$ and $\{kl\}$ from the respective representation matrices for every element of the group. Then these vectors are orthogonal to each other, and their squared norm is equal to the order of the group, divided by the dimension of the irrep*:

$$\sum_{R\in G} \bar{D}^{\Omega}_{ij}(R) D^{\Omega'}_{kl}(R) = \frac{|G|}{\dim(\Omega)} \delta_{\Omega,\Omega'} \delta_{ik} \delta_{jl} \tag{4.45}$$

The theorem thus proceeds as follows: take a given entry ij in the representation matrix of the irrep Ω for every R and order these elements to form a vector of length $|G|$. Do the same with another entry, kl, for a different representation, Ω', and also arrange these to form a vector. Then take the scalar product of these two vectors, bearing in mind that, in this process, the complex conjugate of one of them should be taken (it does not matter which one since the scalar product is always real). The theorem states that this scalar product is zero unless the same irrep is taken, and in this irrep the same row and column index are selected. In that case, the scalar product yields the norm of the vector equal to $|G|/\dim(\Omega)$.

Let us apply this to C_{3v}. For this group, the total number of $\{\Omega, i, j\}$ combinations that can be formed according to the GOT procedure is equal to 6. These

Table 4.2 Complete set of matrix element strings for the group C_{3v}

C_{3v}	$\hat{E}$	$\hat{C}_3$	$\hat{C}_3^2$	$\hat{\sigma}_1$	$\hat{\sigma}_2$	$\hat{\sigma}_3$	$\langle D_{ij}^{\Omega} \vert D_{ij}^{\Omega} \rangle$
A_1	1	1	1	1	1	1	6
A_2	1	1	1	−1	−1	−1	6
E_{11}	1	$-\frac{1}{2}$	$-\frac{1}{2}$	1	$-\frac{1}{2}$	$-\frac{1}{2}$	3
E_{21}	0	$+\frac{\sqrt{3}}{2}$	$-\frac{\sqrt{3}}{2}$	0	$-\frac{\sqrt{3}}{2}$	$+\frac{\sqrt{3}}{2}$	3
E_{12}	0	$-\frac{\sqrt{3}}{2}$	$+\frac{\sqrt{3}}{2}$	0	$-\frac{\sqrt{3}}{2}$	$+\frac{\sqrt{3}}{2}$	3
E_{22}	1	$-\frac{1}{2}$	$-\frac{1}{2}$	−1	$+\frac{1}{2}$	$+\frac{1}{2}$	3

are listed in Table 4.2, based on the matrices in Table 3.2. In general, this number is always equal to the order of the group since, for every irrep, the number of $\{i, j\}$ combinations is equal to the squared dimension of that irrep, and, according to Eq. (4.43), the sum of these squares is equal to $|G|$. The strings in Table 4.2 thus form a set of six linearly independent vectors. This is in accord with our earlier finding that the set of arbitrary functions that form the most general function space for a group has dimension $|G|$. The GOT thus offers the complete list of coefficients from which SALCs may be constructed. How this can be done is shown in the next section. Note that the trace theorem in the previous section is a direct consequence of the GOT that is obtained by taking diagonal matrix entries ii and kk and summing over i and k:

$$\begin{aligned}\left\langle \chi^{\Omega} \vert \chi^{\Omega'} \right\rangle &= \sum_{i,k} \sum_{R \in G} \bar{D}_{ii}^{\Omega}(R) D_{kk}^{\Omega'}(R) \\ &= \frac{|G|}{\dim(\Omega)} \delta_{\Omega,\Omega'} \sum_{ik} \delta_{ik} \\ &= \frac{|G|}{\dim(\Omega)} \delta_{\Omega,\Omega'} \dim(\Omega) \\ &= \delta_{\Omega,\Omega'} |G| \end{aligned} \tag{4.46}$$

4.5 Projection Operators

We recapitulate what we have so far: a group G has been identified, and a function space $|\mathbf{f}\rangle$ was constructed, which is invariant under the action of the group. Next, the characters were determined for each conjugacy class and arranged in a character string, $|\chi\rangle$, which was mapped onto the irreducible characters in the table. Nonzero brackets determined which irreps are present in the function space. Now, the final step is to carry out the actual symmetry adaptation and to obtain the resulting SALCs, say $|\Phi_i^{\Omega}\rangle$. The SALCs are characterized by two indices: the

upper index, Ω, which stands for the irrep, and the lower index, i. The latter index is sometimes called the subrepresentation and also contains a specific piece of information. It determines the component of the irrep, i.e., it refers to a particular column in the irreducible representation matrix that describes the transformation of this component:

$$\hat{R}|\Phi_i^{\Omega}\rangle = \sum_j |\Phi_j^{\Omega}\rangle D_{ji}^{\Omega}(R) \tag{4.47}$$

This symbol of course makes sense only if we do not limit ourselves to the characters, but also determine the representation matrices for all nondegenerate irreps of the group. These will depend on the choice of a particular canonical basis set. Tabular material containing suitable sets of irrep matrices is rather sparse. Some standard choices are provided in Appendix C. Now we construct the projector $\hat{P}$ based on the available matrices:

$$\hat{P}_{kl}^{\Omega'} = \frac{\dim(\Omega')}{|G|} \sum_{R\in G} \bar{D}_{kl}^{\Omega'}(R)\hat{R} \tag{4.48}$$

Let us apply this projector to the SALC $|\Phi_i^{\Omega}\rangle$. This requires the combination of Eqs. (4.47) and (4.48) and exploits the full GOT potential:

$$\begin{aligned}\hat{P}_{kl}^{\Omega'}|\Phi_i^{\Omega}\rangle &= \frac{\dim(\Omega')}{|G|} \sum_{R\in G}\sum_j \bar{D}_{kl}^{\Omega'}(R) D_{ji}^{\Omega}(R)\left|\Phi_j^{\Omega}\right\rangle \\ &= \sum_j \delta_{\Omega',\Omega}\delta_{kj}\delta_{li}\left|\Phi_j^{\Omega}\right\rangle \\ &= \left|\Phi_k^{\Omega'}\right\rangle \delta_{\Omega',\Omega}\delta_{li}\end{aligned} \tag{4.49}$$

The action of the projector entails a twofold selection, both at the level of the representation and of the subrepresentation, indicated by the two Kronecker deltas. First, it compares the irreps of the operator and of the SALC. If they do not match, then the SALC is simply destroyed. Second, the δ_{li} selection rule comes into play—under the "protection," as it were, of the first Kronecker delta, which assures that the second selection rule will matter only when we are already inside the same irrep. This second rule compares index l of the projection operator with index i of the target, and annihilates the target unless they are the same; it therefore selectively picks out the SALC that transforms exactly as the lth component of the Ω' irrep. Third, instead of delivering as result this particular component, the projector also has a built-in ability to act as a ladder operator and turn the lth component so obtained into a kth component. If we do not want this ladder aspect, we simply use the diagonal projection operator with $k = l$. Let us illustrate this for the Q_{Ex} hydrogen bending mode in Fig. 4.2. If we want to obtain from this the Q_{Ey} component, we should use a projection operator that recognizes the x and replaces it by y; hence, it must belong to the E irrep, its row index should be 2, and its column index 1. This

indeed generates the y component of Eq. (4.39):

$$\begin{aligned}\hat{P}^{E}_{21} Q_{E_x} &= \frac{1}{3}\frac{\sqrt{3}}{2}\big[\hat{C}_3 - \hat{C}_3^2 - \hat{\sigma}_2 + \hat{\sigma}_3\big]\frac{1}{\sqrt{2}}(\Delta\phi_C - \Delta\phi_\mathrm{B}) \\ &= \frac{1}{2\sqrt{6}}\big[(\Delta\phi_\mathrm{A} - \Delta\phi_C) - (\Delta\phi_\mathrm{B} - \Delta\phi_\mathrm{A}) \\ &\quad - (-\Delta\phi_\mathrm{A} + \Delta\phi_\mathrm{B}) + (-\Delta\phi_C + \Delta\phi_\mathrm{A})\big] \\ &= \frac{1}{\sqrt{6}}(2\Delta\phi_\mathrm{A} - \Delta\phi_\mathrm{B} - \Delta\phi_C) \\ &= Q_{E_y} \end{aligned} \tag{4.50}$$

For a given irrep, the number of projectors that can be constructed is equal to the number of all possible $\{k, l\}$ combinations, which equals $\dim(\Omega')^2$. By varying the row index, k, one can obtain all the components of the invariance space of a given irrep. This is demonstrated by acting on the operators with an element $\hat{S}$:

$$\begin{aligned}\hat{S}\hat{P}^{\Omega'}_{kl} &= \frac{\dim(\Omega')}{|G|}\sum_{R\in G}\sum_{j}\bar{D}^{\Omega'}_{kl}(R)\hat{S}\hat{R} \\ &= \frac{\dim(\Omega')}{|G|}\sum_{T\in G}\bar{D}^{\Omega'}_{kl}\big(S^{-1}T\big)\hat{T} \\ &= \frac{\dim(\Omega')}{|G|}\sum_{T\in G}\Bigg(\sum_{m}\bar{D}^{\Omega'}_{km}\big(S^{-1}\big)\bar{D}^{\Omega'}_{ml}(T)\Bigg)\hat{T} \\ &= \frac{\dim(\Omega')}{|G|}\sum_{m}D^{\Omega'}_{mk}(S)\Bigg(\sum_{T\in G}\bar{D}^{\Omega'}_{ml}(T)\hat{T}\Bigg) \\ &= \sum_{m}D^{\Omega'}_{mk}(S)\hat{P}^{\Omega'}_{ml} \end{aligned} \tag{4.51}$$

In this derivation we have used the substitution $\hat{S}\hat{R} = \hat{T}$. The result shows that the set of projectors with fixed index l forms a complete basis set for the Ω' irrep. On the other hand, by changing the column index l we have access to different sets of SALCs with the same symmetry. This applies only when the function space has multiplicities, c_Γ, greater than one. This can be illustrated for the $\{|f_R\rangle\}$ function space transforming as the regular representation that has the maximal degree of freedom. Two projectors with the same k index, but different l indices, will project out two functions that are linearly independent, as the following overlap calculation shows:

$$\begin{aligned}\big\langle \hat{P}^{\Omega}_{kl} f_E | \hat{P}^{\Omega}_{kl'} f_E\big\rangle &= \frac{\dim(\Omega)^2}{|G|^2}\Bigg\langle \sum_{R}\bar{D}^{\Omega}_{kl}(R)\hat{R} f_E | \sum_{S}\bar{D}^{\Omega}_{kl}(S)\hat{S} f_E\Bigg\rangle \\ &= \frac{\dim(\Omega)^2}{|G|^2}\sum_{R,S}D^{\Omega}_{kl}(R)\bar{D}^{\Omega}_{kl}(S)\langle f_R | f_S\rangle \end{aligned}$$

$$= \frac{\dim(\Omega)^2}{|G|^2} \sum_{R,S} D^{\Omega}_{kl}(R) \bar{D}^{\Omega}_{kl}(S) \delta_{R,S}$$

$$= \frac{\dim(\Omega)^2}{|G|^2} \sum_{R} D^{\Omega}_{kl}(R) \bar{D}^{\Omega}_{kl'}(R)$$

$$= \frac{\dim(\Omega)}{|G|} \delta_{l,l'} \tag{4.52}$$

Hence, if the multiplicity is greater than one, an additional label preceding the irrep label has to be introduced in order to distinguish SALCs with the same symmetry, and, by varying the l index of the projector, all these can be projected out. Note that the maximal invariance space of a symmetry group is bound to be the regular representation; hence, multiplicities of an invariant function space cannot exceed the dimensions of the irreps and thus will always be covered by the variation of index l. If the multiplicity is smaller than $\dim(\Omega)$, variation of l will give rise to redundancies.

The action of the projector on an arbitrary function can be written as

$$\hat{P}^{\Gamma}_{kl} |f_x\rangle = S^{\Gamma l}_x \left|\Phi^{\Gamma}_k\right\rangle \tag{4.53}$$

Hence, the projector takes out of the function an irreducible part that transforms as the $|\Phi^{\Gamma}_k\rangle$ SALC multiplied by an overlap factor, $S^{\Gamma l}_x$, which indicates the extent to which the $|\Phi^{\Gamma}_l\rangle$ SALC is present in this function. A very concise formulation of this result can be achieved by the use of the Dirac notation. In this notation, the projector is written as

$$\hat{P}^{\Gamma}_{kl} = \left|\Phi^{\Gamma}_k\right\rangle\left\langle\Phi^{\Gamma}_l\right| \tag{4.54}$$

In the ket–bra combination, all the aspects of the projector come together. Let us apply this to our function:

$$\begin{aligned} \hat{P}^{\Gamma}_{kl} |f_x\rangle &= \left|\Phi^{\Gamma}_k\right\rangle\left\langle\Phi^{\Gamma}_l\right|\left|f_x\right\rangle \\ &= \left|\Phi^{\Gamma}_k\right\rangle\left\langle\Phi^{\Gamma}_l\right| f_x\rangle \end{aligned} \tag{4.55}$$

where the convention is followed that the juxtaposition of two vertical lines is contracted to one. Comparing Eqs. (4.54) and (4.55), one can identify the bracket:

$$S^{\Gamma l}_x = \left\langle\Phi^{\Gamma}_l\right| f_x\rangle \tag{4.56}$$

When the projection operator acts (on the left) on a function $|f_x\rangle$, it forms a bracket, which is the overlap factor measuring how much of the $|\Phi^{\Gamma}_l\rangle$ SALC is present in the target. This is the "recognition" part of the projection. It then returns, as a result, the desired SALC $|\Phi^{\Gamma}_k\rangle$ multiplied by the overlap factor. This is the ladder aspect. As an example, consider the action of the $\hat{P}^{E}$ projection operators on the $|1s_{\mathrm{A}}\rangle$ orbital

in ammonia. One has:

$$\begin{aligned}
\hat{P}_{11}|1s_{\mathrm{A}}\rangle &= \frac{1}{3}\big[2|1s_{\mathrm{A}}\rangle - |1s_{\mathrm{B}}\rangle - |1s_{C}\rangle\big] = \frac{\sqrt{2}}{\sqrt{3}}|\psi_x\rangle \\
\hat{P}_{21}|1s_{\mathrm{A}}\rangle &= \frac{\sqrt{2}}{\sqrt{3}}|\psi_y\rangle \\
\hat{P}_{12}|1s_{\mathrm{A}}\rangle &= 0 \\
\hat{P}_{22}|1s_{\mathrm{A}}\rangle &= 0
\end{aligned} \tag{4.57}$$

Note that the bracket $\langle\psi_y|1s_{\mathrm{A}}\rangle$ vanishes because $|1s_{\mathrm{A}}\rangle$ does not occur in the $|\psi_y\rangle$ target, and this gives rise to the zeros in Eq. (4.57). If one wants to avoid the cumbersome construction of the irreducible representation matrices, one can construct trace projectors by putting $k = l$ and summing over all k:

$$\begin{aligned}
\sum_k \hat{P}^{\Gamma}_{kk} &= \frac{\dim(\Gamma)}{|G|}\sum_k\sum_R \bar{D}^{\Gamma}_{kk}(R)\hat{R} \\
&= \frac{\dim(\Gamma)}{|G|}\sum_R \bar{\chi}^{\Gamma}(R)\hat{R}
\end{aligned} \tag{4.58}$$

In this case, only the character tables are needed in order to construct such projectors. They will certainly destroy all parts of the function space that do not belong to the irrep Γ, but, on the other hand, one loses the additional information in the subrepresentation. As we will see in the subsequent chapters, these little auxiliary indices are nonetheless valuable. A further remarkable property of a projector is that if it is applied twice with inverted kl indices, one again obtains a projector:

$$\begin{aligned}
\hat{P}^{\Gamma}_{lk}\hat{P}^{\Gamma}_{kl} &= \frac{\dim(\Gamma)^2}{|G|^2}\sum_{RS}\bar{D}^{\Gamma}_{lk}(R)\bar{D}^{\Gamma}_{kl}(S)\hat{R}\hat{S} \\
&= \frac{\dim(\Gamma)^2}{|G|^2}\sum_{RT}\bar{D}^{\Gamma}_{lk}(R)\bar{D}^{\Gamma}_{kl}\big(R^{-1}T\big)\hat{T} \\
&= \frac{\dim(\Gamma)^2}{|G|^2}\sum_T\sum_m\sum_R\bar{D}^{\Gamma}_{lk}(R)\bar{D}^{\Gamma}_{km}\big(R^{-1}\big)\bar{D}^{\Gamma}_{ml}(T)\hat{T} \\
&= \frac{\dim(\Gamma)^2}{|G|^2}\sum_T\sum_m\Big(\sum_R\bar{D}^{\Gamma}_{lk}(R)D^{\Gamma}_{mk}(R)\Big)\bar{D}^{\Gamma}_{ml}(T)\hat{T} \\
&= \frac{\dim(\Gamma)}{|G|}\sum_T\Big(\sum_m\delta_{m,l}\bar{D}^{\Gamma}_{ml}(T)\Big)\hat{T} \\
&= \hat{P}^{\Gamma}_{ll}
\end{aligned} \tag{4.59}$$

This also implies that the diagonal operator $\hat{P}_{kk}$ is *idempotent*, i.e., applying it twice gives exactly the same result as applying it once:

$$\hat{P}^{\Gamma}_{kk}\hat{P}^{\Gamma}_{kk} = \hat{P}^{\Gamma}_{kk} \tag{4.60}$$

Finally, summing over all diagonal projectors gives rise to the unit element:

$$\sum_{\Gamma}\sum_{i}\hat{P}^{\Gamma}_{ii} = \hat{E} \tag{4.61}$$

The proof is as follows:

$$\begin{aligned}
\sum_{\Gamma}\sum_{i}\hat{P}^{\Gamma}_{ii} &= \frac{1}{|G|}\sum_{\Gamma}\dim(\Gamma)\sum_{i}\sum_{R}\bar{D}^{\Gamma}_{ii}(R)\hat{R} \\
&= \frac{1}{|G|}\sum_{\Gamma}\dim(\Gamma)\sum_{R}\bar{\chi}^{\Gamma}(R)\hat{R} \\
&= \frac{1}{|G|}\sum_{R}\left(\sum_{\Gamma}\dim(\Gamma)\chi^{\Gamma}(R)\right)\hat{R} \\
&= \sum_{R}\delta_{R,E}\hat{R} \\
&= \hat{E}
\end{aligned} \tag{4.62}$$

Here, we have made use of the fact that the sum over all characters multiplied by the dimension of the irrep is the character of the regular representation, and this vanishes for all R except for the unit element, where it is equal to $|G|$ (see Eq. (4.41)). In Dirac terminology this reads

$$\sum_{\Gamma}\sum_{i}\left|\Phi^{\Gamma}_{i}\right\rangle\left\langle\Phi^{\Gamma}_{i}\right| = 1 \tag{4.63}$$

This relation is also known as the *closure* relation. It is frequently applied in the context of the crystal field theory of the lanthanides.

4.6 Subduction and Induction

Many applications are concerned with the reduction of symmetry by external or internal perturbations. Subduction corresponds to the lowering a symmetry group G to one of its subgroups, H, and is denoted by $G \downarrow H$. It can consist of a chain of consecutive symmetry lowerings, following a path of descent in symmetry down the genealogical tree of the group. In physics a typical form of *external* symmetry breaking is through application of a uniform magnetic or electric field. It leads to a subgroup that is the intersection of the molecular point group and the axial or

Table 4.3 Subduction of T_{1u} in $O_h \downarrow D_{3d}$

O_h	$\hat{E}$	$8\hat{C}_3$	$6\hat{C}_2$	$6\hat{C}_4$	$3\hat{C}_2$	$\hat{\imath}$	$6\hat{S}_4$	$8\hat{S}_6$	$3\hat{\sigma}_h$	$6\hat{\sigma}_d$
T_{1u}	3	0	−1	1	−1	−3	−1	0	1	1
D_{3d}	$\hat{E}$	$2\hat{C}_3$	$3\hat{C}_2$			$\hat{\imath}$		$2\hat{S}_6$		$3\hat{\sigma}_d$
T_{1u}	3	0	−1			−3		0		1
A_{2u}	1	1	−1			−1		−1		1
E_u	2	−1	0			−2		1		0

polar symmetry of the applied field, as discussed in Sect. 3.9. In chemistry a common approach to external symmetry breaking is to substitute one or more atoms or atomic groups by homologues, or to interchange sites, which may give rise to different stereo-isomers. *Internal* symmetry breaking is more subtle and may arise as a consequence of the Jahn–Teller effect. In this case the presence of a degenerate electronic state in the high-symmetry conformation of the molecule may provoke a spontaneous geometric distortion of the nuclear frame, leading to a lower symmetry in which the degeneracy is removed. This effect involves the coupling of representations and will be discussed in Sect. 6.6. Our concern here is what will happen to the irreps of G when the symmetry is reduced to H. This can easily be decided on the basis of the character theorem. We simply have to determine the character of the representation in the subgroup. The procedure consists of three steps. One first identifies the correspondence between the elements of G and the elements of H. Then the characters of the irrep in G are transferred to the characters for the corresponding operations in the subgroup. Third, the character string in the subgroup is reduced according to the standard procedure of the character theorem. Hence, let Γ denote an irrep of the parent group, and γ an irrep of the subgroup. The number of times that this subgroup representation occurs in the subduction $G \downarrow H$ is given by

$$c_\gamma(\Gamma G \downarrow H) = \frac{1}{|H|} \sum_{h \in H} \bar{\chi}^\gamma(h) \chi^\Gamma(h) \tag{4.64}$$

In Table 4.3 we follow as an example the fate of the octahedral T_{1u} irrep for the subduction $O_h \downarrow D_{3d}$. When the subduction is performed, the anchoring of the correspondences in the first step of the procedure is very important. For instance, the octahedron has two conjugacy classes of $\hat{C}_2$ axes. The $6\hat{C}_2$ class collects the twofold axes which bisect the Cartesian directions, while the $3\hat{C}_2$ class is made up of the $\hat{C}_4^2$ axes along the Cartesian directions. In the case of subduction to D_{3d}, the three axes perpendicular to the trigonal direction belong to the $6\hat{C}_2$ class. As the table indicates, in D_{3d} the threefold-degenerate representation becomes reducible by splitting into two trigonal irreps:

$$O_h \downarrow D_{3d} : T_{1u} \rightarrow A_{2u} + E_u \tag{4.65}$$

In some cases a subgroup can be reached via two different symmetry breakings. An example is the subduction $O_h \downarrow D_{2h}$. Here, two pathways for symmetry breaking

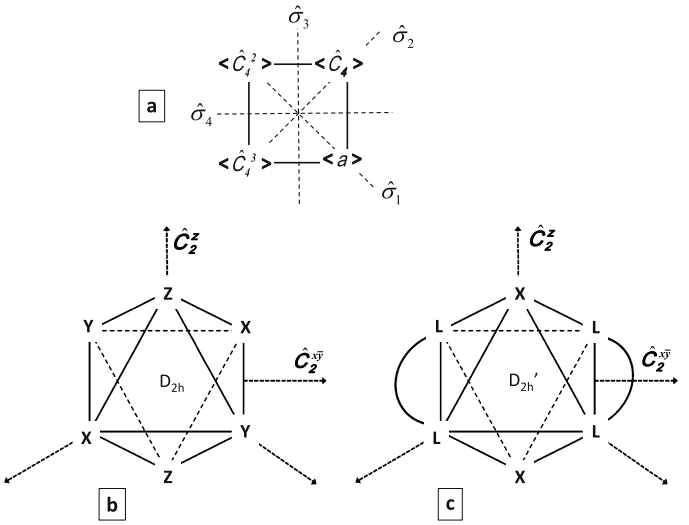

Fig. 4.3 (**a**) generation of equivalent sites in a square starting from $\langle a \rangle$, (**b**) substitutional symmetry lowering of $O_h \downarrow D_{2h}$ in the $MX_2Y_2Z_2$ complex isomer, and (**c**) $O_h \downarrow D'_{2h}$ symmetry lowering by bidentate ligands in *trans*-$M(L-L)_2X_2$

Table 4.4 Subduction of T_{2g} under $O_h \downarrow D_{2h}$

O_h	$\hat{E}$	$3\hat{C}_2$			$\hat{i}$	$3\hat{\sigma}_h$		
D_{2h}	$\hat{E}$	$\hat{C}_2^x$	$\hat{C}_2^y$	$\hat{C}_2^z$	$\hat{i}$	$\hat{\sigma}_{xy}$	$\hat{\sigma}_{xz}$	$\hat{\sigma}_{yz}$
T_{2g}	3	−1	−1	−1	3	−1	−1	−1
B_{1g}	1	−1	−1	1	1	1	−1	−1
B_{2g}	1	−1	1	−1	1	−1	1	−1
B_{3g}	1	1	−1	−1	1	−1	−1	1

are present. The three $\hat{C}_2$ axes of the orthorhombic symmetry are either based on the $3\,\hat{C}_2$ class, $\{\hat{C}_2^x, \hat{C}_2^y, \hat{C}_2^z\}$, or on a mixture of the two classes, as in $\{\hat{C}_2^z, \hat{C}_2^{xy}, \hat{C}_2^{\bar{x}y}\}$. We shall denote the latter group as D'_{2h}. Simple molecular examples of both are shown in Fig. 4.3. Tables 4.4 and 4.5 present the splitting of the T_{2g} irrep over these two subduction paths. The corresponding splitting schemes are as follows:

$$\begin{aligned} O_h \downarrow D_{2h} &: T_{2g} \rightarrow B_{1g} + B_{2g} + B_{3g} \\ O_h \downarrow D'_{2h} &: T_{2g} \rightarrow A_g + B_{2g} + B_{3g} \end{aligned} \tag{4.66}$$

Subduction tables are available in Appendix D.

The opposite process to subduction is induction. Here, we start from an irrep in a subgroup H. By coset expansion, this subgroup is put on an orbit inside a higher symmetry group. This leads to an extension of the function space and generates

Table 4.5 Subduction of T_{2g} under $O_h \downarrow D'_{2h}$

O_h	$\hat{E}$	$6\hat{C}_2$		$3\hat{C}_2$	$\hat{\imath}$	$3\hat{\sigma}_h$	$6\hat{\sigma}_d$	
	$\downarrow$	$\downarrow$	$\searrow$	$\downarrow$	$\downarrow$	$\downarrow$	$\downarrow$	$\searrow$
D'_{2h}	$\hat{E}$	$\hat{C}_2^x$	$\hat{C}_2^y$	$\hat{C}_2^z$	$\hat{\imath}$	$\hat{\sigma}_{xy}$	$\hat{\sigma}_{xz}$	$\hat{\sigma}_{yz}$
T_{2g}	3	1	1	-1	3	-1	1	1
A_g	1	1	1	1	1	1	1	1
B_{2g}	1	-1	1	-1	1	-1	1	-1
B_{3g}	1	1	-1	-1	1	-1	-1	1

irreps of the parent group. The outcome of the induction is determined by the reciprocity theorem due to Frobenius.

Theorem 7 *The number of times that a given irrep Γ of a parent group G occurs in the induction $H \uparrow G$ of a subgroup irrep γ is equal to the number of times that γ is present in the subduction $G \downarrow H$ of that irrep Γ.*

We shall present the proof here since it introduces the important concept of the *ground* representation [2, 3]. This concept is especially useful when considering a polyhedral molecular cluster or complex consisting of several equivalent sites. Typically, these sites could be the atoms in a network covering a hollow cage, or ligands in a metal complex. In the case of ammonia, the sites are simply the three hydrogen atoms. Usually, the site group is of type C_{nv}. We choose site $\langle a \rangle$ as the starting site, which is stabilized by the subgroup H_A. The group G is expanded in cosets of this subgroup, with coset representatives $\hat{g}_\kappa$:

$$G = \sum_\kappa \hat{g}_\kappa H_\mathrm{A} \tag{4.67}$$

As we have seen in the previous chapter, the coset representatives each address a copy of site $\langle a \rangle$, which we shall label as $\langle \kappa \rangle$. The site group that stabilizes this site is isomorphic to H_A and is denoted by H_κ. We thus have the following mappings:

$$\begin{aligned} \langle \kappa \rangle &= \hat{g}_\kappa \langle a \rangle \\ H_\kappa &= \hat{g}_\kappa H_\mathrm{A} \hat{g}_\kappa^{-1} \end{aligned} \tag{4.68}$$

The mapping of the stabilizer, $H_\mathrm{A} \rightarrow H_\kappa$, is recognized as a similarity transformation of the whole subgroup. Two different sites can share the same site group. As an example, in a square pyramidal complex, with parent group C_{4v} and site groups C_s, two ligands, *trans* to each other, have the same site group. With reference to the square in Fig. 4.3a, the cosets may be generated as follows:

$$C_{4v} = \sum_{k=0}^{3} \hat{C}_4^k \{\hat{E}, \hat{\sigma}_1\} = \{\hat{E}, \hat{\sigma}_1\} + \{\hat{C}_4, \hat{\sigma}_4\} + \left\{\hat{C}_4^2, \hat{\sigma}_2\right\} + \left\{\hat{C}_4^3, \hat{\sigma}_3\right\} \tag{4.69}$$

Hence, the four sites of the square are denoted by the coset generators as $\langle a\rangle$, $\langle \hat{C}_4\rangle$, $\langle \hat{C}_4^2\rangle$, and $\langle \hat{C}_4^3\rangle$. Now we also introduce a functional basis on site $\langle a\rangle$, which is represented by the irrep γ, with component labeling m_γ:

$$\hat{h}_{\mathrm{A}}|\gamma m_\gamma; a\rangle = \sum_{m'_\gamma} |\gamma m'_\gamma; a\rangle D^{\gamma}_{m'_\gamma m_\gamma}(h_{\mathrm{A}}) \tag{4.70}$$

The coset generators will once again take this functional space around in an orbit which visits all the equivalent sites. Local basis sets are thus defined as

$$|\gamma m_\gamma; \kappa\rangle = \hat{g}_\kappa |\gamma m_\gamma; a\rangle \tag{4.71}$$

The total induction space is the sum of all these basis sets on the different sites.

As we have seen, the operators of the group act transitively on the cosets. This means that the cosets are permuted among themselves. The permutation matrix is denoted as $\mathbb{P}(g)$. One has

$$\hat{g}(\hat{g}_\kappa H_{\mathrm{A}}) = \sum_\lambda P_{\lambda\kappa}(g)\hat{g}_\lambda H_{\mathrm{A}} \tag{4.72}$$

with

$$\begin{aligned} P_{\lambda\kappa}(g) &= 1 \quad \text{if } \hat{g}(\hat{g}_\kappa H_{\mathrm{A}}) = \hat{g}_\lambda H_{\mathrm{A}} \\ P_{\lambda\kappa}(g) &= 0 \quad \text{if } \hat{g}(\hat{g}_\kappa H_{\mathrm{A}}) \neq \hat{g}_\lambda H_{\mathrm{A}} \end{aligned} \tag{4.73}$$

This permutational representation is also called the *ground* representation. It describes the transformation of the coset space. The dimension of this coset space is $|G|/|H|$. In the case of a cluster, where each coset corresponds to a site, it represents the permutation of the positions of the sites. For this reason, it is also called the *positional* representation. Indeed, Eq. (4.72) may equally well be written as

$$\hat{g}\langle\kappa\rangle = \sum_\lambda P_{\lambda\kappa}(g)\langle\lambda\rangle \tag{4.74}$$

For the λ-value, which marks the position of the nonzero element in the κth column of the matrix $\mathbb{P}$, the product $\hat{g}_\lambda^{-1}\hat{g}\hat{g}_\kappa$ is an element of H_{A}. We call this the *subelement* of $\hat{g}$ in H_{A}. As an example, for the case of the pyramidal complex, the matrices of the positional representation are listed in Table 4.6. If $\hat{g} = \hat{g}_\kappa \hat{h} \hat{g}_\kappa^{-1}$, the diagonal element will be nonzero: $P_{\kappa\kappa}(g) = 1$. The following sum rules will thus hold, as can be verified from Table 4.6:

$$\begin{aligned} \sum_\kappa P_{\kappa\kappa}\left(g_\kappa h g_\kappa^{-1}\right) &= \frac{|G|}{|H|} \\ \sum_{h\in H} P_{\kappa\kappa}\left(g_\kappa h g_\kappa^{-1}\right) &= |H| \end{aligned} \tag{4.75}$$

Table 4.6 Ground or positional representation of the four equatorial ligand sites in a square pyramidal complex; the sites are ordered as in Fig. 4.3(a)

$$\mathbb{P}(E)=\begin{pmatrix}1&0&0&0\\0&1&0&0\\0&0&1&0\\0&0&0&1\end{pmatrix} \qquad \mathbb{P}(\sigma_1)=\begin{pmatrix}1&0&0&0\\0&0&0&1\\0&0&1&0\\0&1&0&0\end{pmatrix}$$

$$\mathbb{P}(C_4)=\begin{pmatrix}0&0&0&1\\1&0&0&0\\0&1&0&0\\0&0&1&0\end{pmatrix} \qquad \mathbb{P}(\sigma_2)=\begin{pmatrix}0&0&1&0\\0&1&0&0\\1&0&0&0\\0&0&0&1\end{pmatrix}$$

$$\mathbb{P}(C_4^2)=\begin{pmatrix}0&0&1&0\\0&0&0&1\\1&0&0&0\\0&1&0&0\end{pmatrix} \qquad \mathbb{P}(\sigma_3)=\begin{pmatrix}0&0&0&1\\0&0&1&0\\0&1&0&0\\1&0&0&0\end{pmatrix}$$

$$\mathbb{P}(C_4^3)=\begin{pmatrix}0&1&0&0\\0&0&1&0\\0&0&0&1\\1&0&0&0\end{pmatrix} \qquad \mathbb{P}(\sigma_4)=\begin{pmatrix}0&1&0&0\\1&0&0&0\\0&0&0&1\\0&0&1&0\end{pmatrix}$$

We are now ready to start the proof. The total induction space is invariant under the operations of the group G. As an example, we can act with an operator of the group on one of the functions on one of the sites:

$$\hat{g}|\gamma m_\gamma;\kappa\rangle=\hat{g}\hat{g}_\kappa|\gamma m_\gamma;a\rangle=\sum_\lambda P_{\lambda\kappa}(g)\hat{g}_\lambda\left[\hat{g}_\lambda^{-1}\hat{g}\hat{g}_\kappa\right]|\gamma m_\gamma;a\rangle \tag{4.76}$$

where we have placed the subelement of $\hat{g}$ in square brackets. This subelement belongs to H_A, under the protection of the $P_{\lambda\kappa}(g)$ prefactor, which will be nonzero only for values of $\hat{g}$ for which this is indeed the case. We can thus introduce the representation matrix for the local on-site transformations:

$$\begin{aligned}\hat{g}|\gamma m_\gamma;\kappa\rangle&=\sum_\lambda\sum_{m'_\gamma}P_{\lambda\kappa}(g)\hat{g}_\lambda|\gamma m'_\gamma;a\rangle D^\gamma_{m'_\gamma m_\gamma}\left(g_\lambda^{-1}gg_\kappa\right)\\&=\sum_\lambda\sum_{m'_\gamma}P_{\lambda\kappa}(g)|\gamma m'_\gamma;\lambda\rangle D^\gamma_{m'_\gamma m_\gamma}\left(g_\lambda^{-1}gg_\kappa\right)\end{aligned} \tag{4.77}$$

This result provides the matrix transformation that shows how the basis functions of the total induction space are transformed under the operations of G. We shall denote this matrix as $\mathbb{D}^{H\uparrow G}$. The structure of this matrix is based on the permutational structure of the ground representation, but the zeros are replaced by small zero blocks of dimension $\dim(\gamma)\times\dim(\gamma)$, and, instead of the ones, the $\mathbb{D}^\gamma(g_\lambda^{-1}gg_\kappa)$ matrices are inserted. A diagonal element of this matrix will be given by $P_{\kappa\kappa}(g)D^\gamma_{m_\gamma m_\gamma}(\hat{g}_\kappa^{-1}\hat{g}\hat{g}_\kappa)$.

Knowing the diagonal elements of the induction matrix, we can now calculate the frequency of a given Γ irrep of the main group, using the character theorem:

$$\begin{aligned} c_\Gamma(\gamma H \uparrow G) &= \frac{1}{|G|}\sum_{g\in G}\bar{\chi}^\Gamma(g)\mathrm{Tr}\left[\mathbb{D}^{H\uparrow G}(g)\right] \\ &= \frac{1}{|G|}\sum_{g\in G}\bar{\chi}^\Gamma(g)\sum_\kappa P_{\kappa\kappa}(g)\chi^\gamma\left(g_\kappa^{-1}gg_\kappa\right) \end{aligned} \tag{4.78}$$

The only elements $\hat{g}$ that are allowed in the summation over κ are the ones such that $(\hat{g}_\kappa^{-1}\hat{g}\hat{g}_\kappa) \in H_\mathrm{A}$. For other elements, $P_{\kappa\kappa}(g)$ are zero. Let us denote by $\hat{h}$ the subelement that allows us to express $\hat{g}$ as

$$\hat{g} = \hat{g}_\kappa\hat{h}\hat{g}_\kappa^{-1} \tag{4.79}$$

Introducing this substitution in Eq. (4.78) yields

$$c_\Gamma(\gamma H \uparrow G) = \frac{1}{|G|}\sum_{h\in H}\sum_\kappa \bar{\chi}^\Gamma\left(g_\kappa h g_\kappa^{-1}\right)\chi^\gamma(h)P_{\kappa\kappa}\left(g_\kappa h g_\kappa^{-1}\right) \tag{4.80}$$

The first character in this equation belongs to the full group and is the same for all elements of a conjugacy class, and hence,

$$\chi^\Gamma\left(g_\kappa h g_\kappa^{-1}\right) = \chi^\Gamma(h) \tag{4.81}$$

Substituting the result of Eq. (4.81) and the sum rule in Eq. (4.75) into the character expression finally gives

$$\begin{aligned} c_\Gamma(\gamma H \uparrow G) &= \frac{1}{|G|}\sum_{h\in H}\sum_\kappa \bar{\chi}^\Gamma(h)\chi^\gamma(h)P_{\kappa\kappa}\left(g_\kappa h g_\kappa^{-1}\right) \\ &= \frac{1}{|G|}\sum_{h\in H}\bar{\chi}^\Gamma(h)\chi^\gamma(h)\left(\sum_\kappa P_{\kappa\kappa}\left(g_\kappa h g_\kappa^{-1}\right)\right) \\ &= \frac{1}{|H|}\sum_{h\in H}\bar{\chi}^\Gamma(h)\chi^\gamma(h) \\ &= c_\gamma(\Gamma G \downarrow H) \end{aligned} \tag{4.82}$$

which concludes the proof. Armed with the subduction tables, we can now read these at once in the opposite sense and obtain the corresponding induction frequencies. As a simple example, consider a hydrogen atom in ammonia. The site symmetry is C_s, and the subduction from C_{3v} reads:

$$\begin{aligned} A_1 &\to a \\ A_2 &\to b \\ E &\to a + b \end{aligned} \tag{4.83}$$

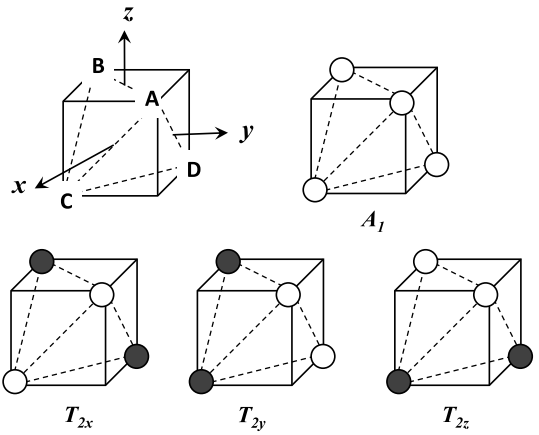

Fig. 4.4 Tetrahedral SALCs in methane. *The open circles* are positive and *the filled circles* are negative. The T_2 orbitals match the sign pattern of central p-orbitals

Using reciprocity, we can thus immediately infer the SALC symmetries of the hydrogen basis functions by selecting the C_{3v} irreps that subduce a in the case of the $1s$ orbitals and b in the case of the bending coordinates:

$$\begin{aligned} \text{Hydrogen } 1s &: aC_s \uparrow C_{3v} = A_1 + E \\ \text{Hydrogen } \Delta\phi &: bC_s \uparrow C_{3v} = A_2 + E \end{aligned} \tag{4.84}$$

Some induction schemes for σ, π, and δ orbital basis sets on C_{nv} sites of polyhedral complexes are to be found in Appendix D. In addition to the Frobenius theorem, there is also a stronger result for induction theory based on the concept of a fiber bundle. This requires the coupling of representations and will be considered in Sect. 6.9.

4.7 Application: The sp^3 Hybridization of Carbon

Methane is the prototype of the saturated aliphatic hydrocarbons. The four hydrogen atoms occupy the corners of a regular tetrahedron, as in Fig. 4.4. Their site symmetry is C_{3v}. The $1s$ atomic orbital on hydrogen is totally symmetric in the site group. The symmetries of the corresponding SALCs can of course be obtained by the standard character procedure, as for the case of ammonia, but we might as well directly obtain them by induction:

$$\Gamma(a_1 C_{3v} \uparrow T_d) = A_1 + T_2 \tag{4.85}$$

The corresponding SALCs can easily be projected:

$$\begin{aligned} &\big(|A_1\rangle \quad |T_{2x}\rangle \quad |T_{2y}\rangle \quad |T_{2z}\rangle\big) \\ &\quad = \big(|1s_{\mathrm{A}}\rangle \quad |1s_{\mathrm{B}}\rangle \quad |1s_C\rangle \quad |1s_D\rangle\big) \times \mathbb{T} \end{aligned} \tag{4.86}$$

with

$$\mathbb{T} = \frac{1}{2}\begin{pmatrix} 1 & 1 & 1 & 1 \\ 1 & -1 & -1 & 1 \\ 1 & 1 & -1 & -1 \\ 1 & -1 & 1 & -1 \end{pmatrix} \tag{4.87}$$

SALCs are normalized to unity, neglecting overlap between the sites. The matrix $\mathbb{T}$ transforms the localized orbitals on the sites to delocalized molecular orbitals with irreducible symmetry characteristics. The inverse matrix $\mathbb{T}^{-1}$ fulfills the opposite role and localizes the molecular orbital set back on the atomic sites.

The valence shell of the central carbon atom contains four orbitals, which incidentally also transform as $A_1 + T_2$. The precise correspondence is as follows:

$$\begin{aligned} |2s\rangle &\leftrightarrow A_1 \\ |2p_x\rangle &\leftrightarrow T_{2x} \\ |2p_y\rangle &\leftrightarrow T_{2y} \\ |2p_z\rangle &\leftrightarrow T_{2z} \end{aligned} \tag{4.88}$$

Hence, we can match the central valence shell with the hydrogen SALCs. In fact, this correspondence provides a simple pictorial method for obtaining the SALCs immediately. The weighting coefficients for a given SALC are simply taken as proportional to the local amplitude of the central $2s$ or $2p$ function, with the same symmetry, as is illustrated in Fig. 4.4. In this way one obtains a SALC that has the same nodal characteristics and thus the same symmetry as the central orbital. Note that this procedure also aligns the phases of the peripheral and central orbitals.

Starting from on-site localized atomic orbitals, we have thus transformed these into SALCs using the $\mathbb{T}$ matrix and then found a perfect matching with the central valence orbitals on carbon. What would now be the effect of applying the inverse transformation, $\mathbb{T}^{-1}$, not to the hydrogen SALCs but to the central carbon orbitals? This yields an interesting result. The inverse matrix, which transforms delocalized SALCs back into localized orbitals, reshapes the carbon valence orbitals by projecting out linear combinations, of mixed or *hybrid* character, which are maximally directed to a single site of the tetrahedron. These are the ubiquitous sp^3 hybrids of Pauling, which we can label with the site labels A, B, C, and D:

$$\begin{aligned} &\left(|sp^3_{\mathrm{A}}\rangle \quad |sp^3_{\mathrm{B}}\rangle \quad |sp^3_{C}\rangle \quad |sp^3_{D}\rangle\right) \\ &\quad = \left(|2s\rangle \quad |2p_x\rangle \quad |2p_y\rangle \quad |2p_z\rangle\right)\frac{1}{2}\begin{pmatrix} 1 & 1 & 1 & 1 \\ 1 & -1 & 1 & -1 \\ 1 & -1 & -1 & 1 \\ 1 & 1 & -1 & -1 \end{pmatrix} \end{aligned} \tag{4.89}$$

The components of the valence shell of carbon being a scalar ($2s$) and a vector ($2p$), the tetrahedron is the optimal geometry that provides four valence sites, which together transform precisely as scalar and vector. The alternative high-symmetry

four-site structure is the square, but, from the tables in Appendix D, the induction from the C_{2v} sites in a square-planar structure yields

$$\Gamma(a_1 C_{2v} \uparrow D_{4h}) = A_{1g} + B_{2g} + E_u \tag{4.90}$$

This matches the symmetry of sp^2d hybrids. It is thus not suitable for carbon, but indeed describes the valence structure of square-planar transition-metal complexes where d-orbitals are involved in the bonding.

4.8 Application: The Vibrations of UF_6

As we have already mentioned, representations not only apply to orbitals, but equally well to vibrational coordinates. The function space in such a case consists of a set of distortions. When applying symmetry operations we do not move the atoms, but the distortions. Let us consider the vibrations of an octahedral complex, such as UF_6, which can be brought into the gas phase and which has been studied in great detail since it is the carrier of uranium in the gas diffusion process for enrichment of nuclear fuel. The atoms are labeled as in Fig. 4.5, and on each atom we define a local coordinate system that parallels the central system. In the notation adopted, ΔY_2 is a variable for a displacement of atom 2 over a distance Δ in the positive y-direction. A symmetry operation such as $\hat{C}_4^z$ transforms this ΔY_2 into $-\Delta X_3$. The seven atoms give rise to 21 distortions, which include six spurious modes, corresponding to three translations and three rotations. The seven atoms form two different orbits: the orbit containing the six fluoride ligands and the one-atom orbit of the central uranium atom. The displacements of one ligand can further be separated into a radial or σ-mode and two tangential or π-modes, which, in the C_{4v} site group, transform as a_1 and e, respectively. Altogether, the distortion space thus contains three different basis sets: the central atom, the ligand σ-modes, and the ligand π-modes. For each of these, the symmetry content may be determined by directly applying the character theorem, or—for the case of the ligands—by using induction. The three displacements of the uranium atom transform as the T_{1u} irrep of the central translation mode. The ligand inductions are as follows:

$$\begin{aligned} \mathrm{F}\sigma &: \Gamma(a_1 C_{4v} \uparrow O_h) = A_{1g} + E_g + T_{1u} \\ \mathrm{F}\pi &: \Gamma(eC_{4v} \uparrow O_h) = T_{1g} + T_{2g} + T_{1u} + T_{2u} \end{aligned} \tag{4.91}$$

We can now determine the symmetry-adapted coordinates by applying the projection operators, but the results can be written down almost immediately by again using the criterion of overlap with central symmetry functions. The A_{1g}, T_{1u}, and $E_g + T_{2g}$ SALCs reflect the nodal patterns of central s, p, and d functions, respectively. The T_{1g} mode corresponds to the rotation and evidently consists of tangential displacements of ligands in the equator perpendicular to the rotation axis. Finally, the T_{2u} is a buckling mode, which has the symmetry of central f orbitals, viz.

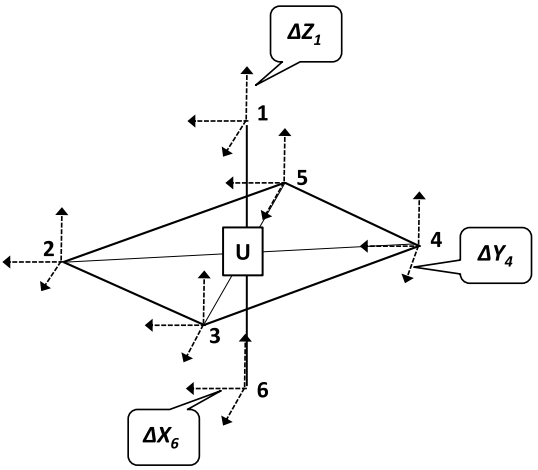

Fig. 4.5 Ligand numbering and displacement coordinates for UF_6

Table 4.7 Symmetry coordinates for UF_6

$UT_{1u}p_x$	ΔX_0
$UT_{1u}p_y$	ΔY_0
$UT_{1u}p_z$	ΔZ_0
$F\sigma A_{1g}s$	$1/\sqrt{6}(\Delta Z_1 + \Delta X_2 + \Delta Y_3 - \Delta X_4 - \Delta Y_5 - \Delta Z_6)$
$F\sigma E_g d_{z^2}$	$1/\sqrt{12}(2\Delta Z_1 - \Delta X_2 - \Delta Y_3 + \Delta X_4 + \Delta Y_5 - 2\Delta Z_6)$
$F\sigma E_g d_{x^2-y^2}$	$1/2(\Delta X_2 - \Delta Y_3 - \Delta X_4 + \Delta Y_5)$
$F\sigma T_{1u}p_x$	$1/\sqrt{2}(\Delta X_2 + \Delta X_4)$
$F\sigma T_{1u}p_y$	$1/\sqrt{2}(\Delta Y_3 + \Delta Y_5)$
$F\sigma T_{1u}p_z$	$1/\sqrt{2}(\Delta Z_1 + \Delta Z_6)$
$F\pi T_{1g}x$	$1/2(-\Delta Y_1 + \Delta Z_3 - \Delta Z_5 + \Delta Y_6)$
$F\pi T_{1g}y$	$1/2(\Delta X_1 - \Delta Z_2 - \Delta X_6 + \Delta Z_4)$
$F\pi T_{1g}z$	$1/2(\Delta Y_2 - \Delta X_3 - \Delta Y_4 + \Delta X_5)$
$F\pi T_{2g}d_{yz}$	$1/2(\Delta Y_1 + \Delta Z_3 - \Delta Z_5 - \Delta Y_6)$
$F\pi T_{2g}d_{xz}$	$1/2(\Delta X_1 + \Delta Z_2 - \Delta X_6 - \Delta Z_4)$
$F\pi T_{2g}d_{xy}$	$1/2(\Delta Y_2 + \Delta X_3 - \Delta Y_4 - \Delta X_5)$
$F\pi T_{1u}p_x$	$1/2(\Delta X_1 + \Delta X_3 + \Delta X_5 + \Delta X_6)$
$F\pi T_{1u}p_y$	$1/2(\Delta Y_1 + \Delta Y_2 + \Delta Y_4 + \Delta Y_6)$
$F\pi T_{1u}p_z$	$1/2(\Delta Z_2 + \Delta Z_3 + \Delta Z_4 + \Delta Z_5)$
$F\pi T_{2u}f_{x(y^2-z^2)}$	$1/2(-\Delta X_1 + \Delta X_3 + \Delta X_5 - \Delta X_6)$
$F\pi T_{2u}f_{y(z^2-x^2)}$	$1/2(\Delta Y_1 - \Delta Y_2 - \Delta Y_4 + \Delta Y_6)$
$F\pi T_{2u}f_{z(x^2-y^2)}$	$1/2(\Delta Z_2 - \Delta Z_3 + \Delta Z_4 - \Delta Z_5)$

$f_{z(x^2-y^2)}$, and its cyclic permutations $f_{x(y^2-z^2)}$ and $f_{y(z^2-x^2)}$. In Table 4.7 we list all 21 symmetry coordinates by category, using labels that refer to the central harmonic functions. We may denote the 21 symmetry coordinates by a row vector **S**.

The kinetic energy is then given by

$$T = \frac{1}{2}\sum_{i=1}^{21} m_i \left(\frac{\mathrm{d}S_i}{\mathrm{d}t}\right)^2$$
$$= \frac{M}{2}\sum_{i=1}^{3}\left(\frac{\mathrm{d}S_i}{\mathrm{d}t}\right)^2 + \frac{m}{2}\sum_{i=4}^{21}\left(\frac{\mathrm{d}S_i}{\mathrm{d}t}\right)^2 \tag{4.92}$$

Here, M is the atomic mass of uranium, and m is the atomic mass of fluorine. The kinetic energy can be reduced to a uniform scalar product by mass weighting the coordinates, i.e., by multiplying the S coordinates with the square root of the atomic mass of the displaced atom. We shall denote these as the vector $\mathbf{Q}$. Hence, $Q_i = \sqrt{m_i}S_i$:

$$T = \frac{1}{2}\sum_i \left(\frac{\mathrm{d}Q_i}{\mathrm{d}t}\right)^2 = \frac{1}{2}\sum_i \dot{Q}_i^2 \tag{4.93}$$

where the dot over Q denotes the time derivative. The potential energy will be approximated by second-order derivatives of the potential energy surface $V(\mathbf{Q})$ in the mass-weighted coordinates:

$$V_{ij} = \frac{\partial^2 V}{\partial Q_i \partial Q_j} \tag{4.94}$$

These derivatives are the elements of the Hessian matrix, $\mathbb{V}$, which is symmetric about the diagonal. The potential minimum coincides with the octahedral geometry. The resulting potential energy is

$$V = \frac{1}{2}\sum_{i,j} V_{ij} Q_i Q_j \tag{4.95}$$

The kinetic and potential energies are combined to form the Lagrangian, $L = T - V$. The equation of motion is given by

$$\frac{\partial L}{\partial Q_k} = \frac{\mathrm{d}}{\mathrm{d}t}\frac{\partial L}{\partial \dot{Q}_k} \tag{4.96}$$

The partial derivatives in this equation are given by

$$\frac{\partial L}{\partial Q_k} = -\frac{\partial V}{\partial Q_k} = -V_{kk}Q_k - \frac{1}{2}\sum_{i\neq k}(V_{ik}+V_{ki})Q_i$$
$$= -V_{kk}Q_k - \sum_{i\neq k} V_{ki}Q_i = -\sum_i V_{ki}Q_i \tag{4.97}$$

$$\frac{\mathrm{d}}{\mathrm{d}t}\frac{\partial L}{\partial \dot{Q}_k} = \frac{\mathrm{d}}{\mathrm{d}t}\frac{\partial T}{\partial \dot{Q}_k} = \frac{\mathrm{d}}{\mathrm{d}t}\dot{Q}_k = \ddot{Q}_k \tag{4.98}$$

Table 4.8 Vibrational spectrum of UF_6

Symmetry	Type	$\bar{\nu}(\mathrm{cm}^{-1})$	Calc.	Technique
$\nu_1(A_{1g})$	Breathing	667	669	Raman (very strong)
$\nu_2(E_g)$	Stretching	533	534	Raman (weak)
$\nu_3(T_{1u})$	Stretching	626	624	IR
$\nu_4(T_{1u})$	Bending	186	181	IR
$\nu_5(T_{2g})$	Bending	202	191	Raman (weak)
$\nu_6(T_{2u})$	Buckling	142	140	Overtone

It will be assumed that the coordinates vary in a harmonic manner with an angular frequency ω; hence, $Q_k = Q_k^{\max} \cos \omega t$. The second derivative is then given by

$$\ddot{Q}_k = -\omega^2 Q_k = -(2\pi \nu)^2 Q_k \tag{4.99}$$

where ν is the vibrational frequency in Hertz. The equation of motion then is turned into a set of homogeneous linear equations:

$$\forall k: \quad \sum_i \left(V_{ki} - \delta_{ki}\omega^2\right) Q_i = 0 \tag{4.100}$$

This set of equations is solved in the standard way by diagonalizing the Hessian matrix, as

$$\left|\mathbb{V} - \omega^2 \mathbb{I}\right| = 0 \tag{4.101}$$

The eigenvalues of the secular equation yield the frequencies of the normal modes, which are usually expressed as wavenumbers, $\bar{\nu}$, preferentially in reciprocal centimetres, cm^{-1} by dividing the frequency by the speed of light, c.

$$\bar{\nu} = \frac{\nu}{c} = \frac{\omega}{2\pi c} \tag{4.102}$$

In Table 4.8 we present the experimental results [4] for $U^{238}F_6$, as compared with the Hessian eigenvalues, based on extensive relativistic calculations [5]. The eigenfunctions of the Hessian matrix are the corresponding normal modes. The Hessian matrix will be block-diagonal over the irreps of the group and, within each irrep, over the individual components of the irrep. Moreover, the blocks are independent of the components. All this illustrates the power of symmetry, and the reasons for it will be explained in detail in the next chapter. As an immediate consequence, symmetry coordinates, which belong to irreps that occur only once, are exact normal modes of the Hessian. Five irreps fulfil this criterion: the T_{1g} mode, which corresponds to the overall rotations, and the vibrational modes, $A_{1g} + E_g + T_{2g} + T_{2u}$. Only the T_{1u} irrep gives rise to a triple multiplicity. In this case, the actual normal modes will depend on the matrix elements in the Hessian. Let us study this in detail

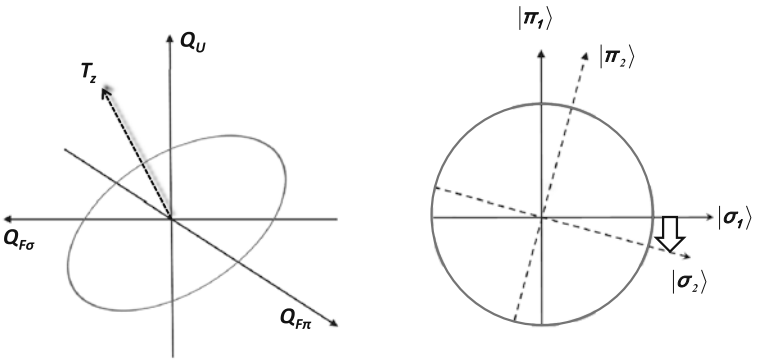

Fig. 4.6 T_{1u} distortion space for UF_6 with coordinates as defined in Eq. (4.103); T_z is the translation of mass. The circle, perpendicular to this direction, is the space of vibrational stretching and bending, with coordinates defined in Eqs. (4.104) and (4.105). The angle $\langle\sigma_2|\sigma_1\rangle$ is $-10.5°$

for the three $T_{1u}z$-components, which we shall abbreviate as follows:

$$\begin{aligned} Q_{\mathrm{U}} &= \sqrt{M}\,\Delta Z_0 \\ Q_\sigma &= \frac{\sqrt{m}}{\sqrt{2}}(\Delta Z_1 + \Delta Z_6) \\ Q_\pi &= \frac{\sqrt{m}}{2}(\Delta Z_2 + \Delta Z_3 + \Delta Z_4 + \Delta Z_5) \end{aligned} \tag{4.103}$$

This space is still reducible since it includes the translation in the z-direction. The translation coordinate corresponds to the displacement of the center of mass in the z-direction. It is given by $\sum_i m_i \Delta Z_i$, which can be expressed as follows:

$$\begin{aligned} T_z &= M\Delta Z_0 + m(\Delta Z_1 + \Delta Z_2 + \Delta Z_3 + \Delta Z_4 + \Delta Z_5 + \Delta Z_6) \\ &= \sqrt{M}\,Q_{\mathrm{U}} + \sqrt{2m}\,Q_\sigma + \sqrt{4m}\,Q_\pi \end{aligned} \tag{4.104}$$

We can remove this degree of freedom from the function space by a standard orthogonalization procedure. One option is to construct first a pure stretching mode, which does not involve the Q_π coordinate. This mode is denoted by $|\sigma_1\rangle$. The remainder of the function space, which is orthogonal both to the translation and to this pure stretching mode, is then denoted by $|\pi_1\rangle$. Normalizing these modes with respect to mass-weighted coordinates yields:

$$\begin{aligned} |\sigma_1\rangle &= \frac{-\sqrt{2m}\,Q_{\mathrm{U}} + \sqrt{M}\,Q_\sigma}{\sqrt{M+2m}} \\ |\pi_1\rangle &= \frac{-\sqrt{4mM}\,Q_{\mathrm{U}} - m\sqrt{8}\,Q_\sigma + (M+2m)\,Q_\pi}{\sqrt{(M+2m)(M+6m)}} \end{aligned} \tag{4.105}$$

An alternative option would be to construct a pure bending mode, based on the tangent motions. Let us denote this by $|\pi_2\rangle$. The remainder is then denoted by $|\sigma_2\rangle$.

$$\begin{aligned} |\sigma_2\rangle &= \frac{-\sqrt{2mM}\,Q_{\mathrm{U}} + (M+4m)\,Q_\sigma - m\sqrt{8}\,Q_\pi}{\sqrt{(M+4m)(M+6m)}} \\ |\pi_2\rangle &= \frac{-\sqrt{4m}\,Q_{\mathrm{U}} + \sqrt{M}\,Q_\pi}{\sqrt{M+4m}} \end{aligned} \tag{4.106}$$

In Fig. 4.6 we present both choices of bases. The angle, α, between both basis sets is defined by

$$\cos\alpha = \sqrt{\frac{M(M+6m)}{(M+2m)(M+4m)}} \tag{4.107}$$

In the case of UF_6 ($m = 18.998$, $M = 238.050$) this angle is $-10.5°$. The actual eigenmodes are found by setting up the Hessian in one of these coordinate sets and diagonalizing it. This Hessian matrix is symmetric and thus contains three independent parameters: the two diagonal elements and the single off-diagonal element. The sum of the resulting eigenvalues is equal to the trace of the matrix, and the product is equal to its determinant; this leaves still one degree of freedom, which can be associated with the *composition* of the normal mode, viz. the angle of rotation in the diagram. It is important to realize that this composition also gives rise to observables, albeit not the eigenfrequencies, but a variety of other properties, such as the intensities of the vibrational transition, isotope shifts and isotope splittings, or electron diffraction amplitudes. For most octahedral complexes, as in the case of UF_6, the rotation angle for the actual T_{1u} eigenmodes lies in the interval $[0, \alpha]$. This means that the modes may approximately be assigned as a stretching and a bending mode. In the spectrum their frequencies are denoted as ν_3 and ν_4, respectively. The isotope effect of the radioactive nucleus U^{235}, as distinct from U^{238}, is absent for all modes, except for the T_{1u} modes, since these involve the displacement of uranium. Of the latter two, the strongest effect is expected for the stretching vibration, since this involves the largest displacement of the central atom. The pure stretching mode, $|\sigma_1\rangle$, can be expressed in terms of the displacements along the z-direction as

$$|\sigma_1\rangle = \sqrt{\frac{2mM}{M+2m}}\left(-\Delta Z_0 + \frac{\Delta Z_1 + \Delta Z_6}{2}\right) \tag{4.108}$$

This is precisely the antisymmetric mode for a triatomic F–U–F oscillator. The square root preceding the modes corresponds to a mass weighting by the reduced mass, μ, for such an oscillator:

$$\mu = \left(\frac{1}{M} + \frac{1}{2m}\right)^{-1} = \frac{2mM}{M+2m} \tag{4.109}$$

Substitution of U^{238} by the U^{235} isotope will reduce this effective mass by a factor 0.9982. The frequency is accordingly increased by the square root of this factor.

This gives an increase of frequency of 0.56 cm^{-1}, which is close to the experimental value [6] of 0.60 cm^{-1}. This confirms the dominant stretching character of the ν_3 mode.

What have we learned from this example? The Hessian matrix is block diagonal over the irreps of the point group, and, as a result, the normal modes are characterized by symmetry labels. These labels are exact spectral assignments. In the long run their relevance for the study of symmetry may be more important than the temporary gain in computational time for evaluation and diagonalization of the Hessian matrix.

4.9 Application: Hückel Theory

The Hückel model for the chemist (or the analogous tight-binding model for the condensed-matter physicist) is an extremely simplified molecular orbital model [7], which nevertheless continues to play an important role in our understanding of electronic structures and properties. It emphasizes the molecule–graph analogy and uses what is now regarded as spectral graph theory [8, 9] in order to obtain molecular orbitals. Its strength comes from the fact that, in spite of the approximations involved, it incorporates the essential topological and symmetry aspects of electronic structures, and, as we keep repeating, these are simple but exact properties of complex molecular quantum-systems. Hückel theory is preferentially applied to molecular systems where each atom or node carries one atomic orbital, say $|\phi_i\rangle$. Molecular orbitals will be denoted as $|\Phi_k\rangle$. To find the molecular orbitals, one sets up the Hückel Hamiltonian matrix, which in its most simplified form is proportional to the adjacency matrix, $\mathbb{A}$, of the molecular graph. Elements of the adjacency matrix are zero, unless row and column index refer to neighboring nodes, in which case the matrix element is equal to one. The Hamiltonian matrix then is given by

$$\langle\phi_i|\mathcal{H}|\phi_j\rangle = \alpha\delta_{ij} + \beta A_{ij} \tag{4.110}$$

or, in operator form,

$$\mathcal{H} = \sum_i \alpha|\phi_i\rangle\langle\phi_i| + \sum_{i\neq j} \beta A_{ij}|\phi_i\rangle\langle\phi_j| \tag{4.111}$$

Here, α is the so-called Coulomb integral, which corresponds to the on-site interaction element. It defines the zero-point of energy and thus has only a symbolic significance in homogeneous systems. However, in hetero-atomic systems, it is important to differentiate the atoms. As an example, the Coulomb integral for nitrogen will be more negative than the one for carbon because the heavier nitrogen nucleus exerts a greater attraction on the electrons. The β parameter is the resonance or inter-site hopping integral. It represents a bonding interaction and thus is negative. The Hückel eigenvalues are thus of opposite sign as compared with the corresponding eigenvalues of the adjacency matrix. The molecular symmetry group is called in

to transform the atomic basis into SALCs according to the irreps of the point group. Molecular orbitals have a definite irrep and component symmetry and thus contain only SALCs with these same symmetry characteristics. Transforming the atomic basis into SALCs will reduce the Hamiltonian matrix to a set of smaller symmetry blocks. From the eigenfunctions one can determine π-contributions to properties such as the on-site atomic population, q_r, and the inter-site π-bond order, p_{rs}. The population of atom r and the bond order of the bond between atoms r and s are given by

$$\begin{aligned} q_r &= \sum_k n_k |c_r^k|^2 \\ p_{rs} &= \sum_k n_k \overline{c_r^k} c_s^k \end{aligned} \tag{4.112}$$

Here, the index k runs over the eigenfunctions: n_k is the occupation number (0,1, or 2) of the kth eigenlevel, and c_r^k is the coefficient of the $|\phi_r\rangle$ atomic orbital for the normalized eigenfunction. The atomic populations are simply the densities or weights at the atomic sites and may vary between 0 and 2. The neutral atom has a population of one p_z-electron, and sites with $q_r < 1$ are cationic and with $q_r > 1$ anionic. The bond order adopts the form of a correlation coefficient between two sites. The π-bond order for a full π-bond in ethylene is equal to 1, and for benzene, it is $2/3$. Below we shall examine in detail some special cases where symmetry plays an important role.

Cyclic Polyenes

Cyclic polyenes, also known as *annulenes*, are hydrocarbon rings, C_nH_n. Each carbon atom contributes one p_z-orbital, perpendicular to the plane of the ring, which gives rise to conjugated π-bonding. The prototype is the aromatic molecule benzene. The adjacency matrix has the form of a *circulant* matrix. This is a matrix where each row is rotated one element to the right relative to the preceding row. Because each atom is linked to only two neighbors, each row contains only two elements. These are arranged left and right of the diagonal, which is characteristic for a chain, but with additional nonzero elements in the upper right and lower left corners, where both ends of the chain meet. For benzene, it is given by

$$\mathbb{A} = \begin{pmatrix} 0 & 1 & 0 & 0 & 0 & 1 \\ 1 & 0 & 1 & 0 & 0 & 0 \\ 0 & 1 & 0 & 1 & 0 & 0 \\ 0 & 0 & 1 & 0 & 1 & 0 \\ 0 & 0 & 0 & 1 & 0 & 1 \\ 1 & 0 & 0 & 0 & 1 & 0 \end{pmatrix} \tag{4.113}$$

The symmetry of an N-atom ring is D_{Nh}, but in practice the cyclic group C_N is sufficient to solve the eigenvalue problem. Atoms are numbered from 0 to $N-1$. The cyclic projection operator, $\hat{P}_k$, is given by

$$\hat{P}_k = \frac{1}{N}\sum_{j=0}^{N-1} \exp\left(2\pi i \frac{jk}{N}\right)\hat{C}_N^j \tag{4.114}$$

Projectors are characterized by an integer k in a periodic interval. We may choose the range $]-N/2, +N/2]$ as the standard interval. The total number of integers in this interval is N. Keeping in mind the active view, where the rotation axis will rotate all the orbitals one step further in a counterclockwise way, we now act with the projection operator on the starting orbital, $|\phi_0\rangle$:

$$\hat{P}_k|\phi_0\rangle = \frac{1}{N}\sum_{j=0}^{N-1} \exp\left(2\pi i \frac{jk}{N}\right)|\phi_j\rangle \tag{4.115}$$

The result is an unnormalized SALC, which we denote as $|\Phi_k\rangle$. Neglecting overlap between adjacent atoms, we obtain the normalized SALC as

$$|\Phi_k\rangle = \sqrt{N}\,\hat{P}_k|\phi_0\rangle \tag{4.116}$$

The transformation properties of this SALC under the rotation axis are characterized as

$$\begin{aligned}\hat{C}_N|\Phi_k\rangle &= \frac{1}{\sqrt{N}}\sum_{j=0}^{N-1} \exp\left(2\pi i \frac{jk}{N}\right)|\phi_{j+1}\rangle \\ &= \frac{1}{\sqrt{N}}\sum_{j=0}^{N-1} \exp\left(2\pi i \frac{(j-1)k}{N}\right)|\phi_j\rangle \\ &= \exp\left(-2\pi i \frac{k}{N}\right)|\Phi_k\rangle\end{aligned} \tag{4.117}$$

Applying this symmetry element N times is identical to the unit operation and raises the exponential factor in this expression to the Nth power:

$$\left(\exp\left(-2\pi i \frac{k}{N}\right)\right)^N = \exp(-2\pi i k) = 1 \tag{4.118}$$

Each integer value of k in the periodic interval $]-N/2, +N/2]$ thus characterizes a different SALC. The corresponding energy eigenvalues are also easily extracted:

$$\begin{aligned}E_k &= \langle\Phi_k|\mathcal{H}|\Phi_k\rangle \\ &= \frac{1}{N}\sum_{j,j'=0}^{N-1} \exp\left(2\pi i \frac{k(-j+j')}{N}\right)\langle\phi_j|\mathcal{H}|\phi_{j'}\rangle\end{aligned}$$

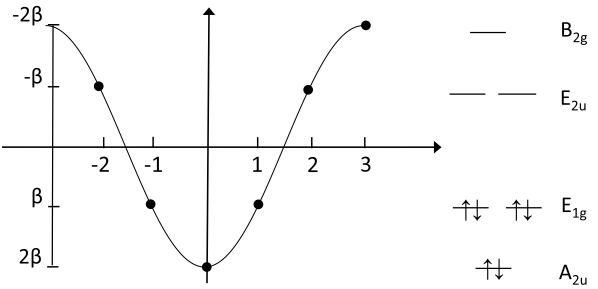

Fig. 4.7 Hückel orbital energy spectrum of benzene as a function of index k, with allowed values $0, \pm 1, \pm 2, 3$

$$= \frac{1}{N} \sum_{j=0}^{N-1} \left(\alpha + \beta\left[\exp(-2\pi i k/N) + \exp(+2\pi i k/N)\right]\right)$$

$$= \alpha + 2\beta \cos(2\pi k/N) \tag{4.119}$$

The energies are thus seen to form N discrete levels, which are points on a cosine curve, as shown in Fig. 4.7. Except for $k = 0$, and in the case of N even, $k = N/2$, all levels E_k and E_{-k} are twofold-degenerate. Closed-shell structures thus will be realized for $N = 4n + 2$, which is the famous Hückel condition for aromaticity. These cyclic labels can easily be expanded to the full irrep designations of the D_{6h} symmetry group for benzene. The atomic p_z-orbitals transform as b_1 in the C_{2v} site group. In accord with the conventions for the D_{6h} point group symmetry, as pictured in Fig. 3.10, this site group is based on operators of type $\hat{C}_2'$ and $\hat{\sigma}_v$. The induced irrep of the six atomic orbitals then becomes

$$\Gamma(b_1 C_{2v} \uparrow D_{6h}) = A_{2u} + E_{1g} + E_{2u} + B_{2g} \tag{4.120}$$

Since each irrep occurs only once, there is a one-to-one correlation between these irreps and the cycle index k, which can be retrieved from the $D_{6h} \downarrow C_6$ subduction rules :

$$\begin{aligned} A_{2u} &\longrightarrow A \quad (k = 0) \\ E_{1g} &\longrightarrow E_1 \quad (k = \pm 1) \\ E_{2u} &\longrightarrow E_2 \quad (k = \pm 2) \\ B_{2g} &\longrightarrow B \quad (k = 3) \end{aligned} \tag{4.121}$$

We will now engage in a more elaborate application of Hückel theory, which demonstrates the power of this simple model. The purpose is to determine the energy shifts of the eigenvalues when an annulene is brought into a uniform magnetic field, **B**. This field is independent of position and time. It can be defined as the "curl" (or rotation) of a vector potential **A**, and, in terms of a position vector **r** from a given

origin, the relevant relations are as follows:

$$\begin{aligned}\mathbf{B} &= \nabla \wedge \mathbf{A} \\ \mathbf{A} &= \frac{1}{2}\mathbf{B} \wedge \mathbf{r}\end{aligned} \tag{4.122}$$

This implies that the divergence of the vector potential is zero, and hence $\mathbf{A}$ and ∇ commute: $[\nabla, \mathbf{A}] = \mathbf{0}$. The introduction of the magnetic field will add an extra term in the kinetic energy operator, which becomes

$$\begin{aligned}T &= \frac{1}{2m}\left(\frac{\hbar}{i}\nabla + \mathrm{e}\mathbf{A}\right)^2 \\ &= -\frac{h^2}{8\pi^2 m}\left(\nabla + i\frac{\mathrm{e}}{\hbar}\mathbf{A}\right)^2 \\ &= -\frac{h^2}{8\pi^2 m}\left(\Delta + i\frac{\mathrm{e}}{\hbar}\mathbf{A}\cdot\nabla + i\frac{\mathrm{e}}{\hbar}\nabla\cdot\mathbf{A} - \frac{\mathrm{e}^2}{\hbar^2}A^2\right) \\ &= -\frac{h^2}{8\pi^2 m}\left(\Delta + 2i\frac{\mathrm{e}}{\hbar}\mathbf{A}\cdot\nabla - \frac{\mathrm{e}^2}{\hbar^2}A^2\right)\end{aligned} \tag{4.123}$$

where we have taken into account that the "del" (or nabla) operator and the vector potential commute. The electron charge is $-\mathrm{e}$. London proposed that the atomic basis functions should be multiplied by a phase factor, which explicitly depends on the vector potential [10]. In this London gauge the atomic orbitals are rewritten as

$$|\chi_j\rangle = \exp\left(-i\frac{\mathrm{e}}{\hbar}\mathbf{A}_j\cdot\mathbf{r}\right)|\phi_j\rangle \tag{4.124}$$

where $\mathbf{A}_j$ is the vector potential at the position of the jth atom. The effect of this phase factor is to move the origin of the vector potential from an arbitrary origin to the local position of atom j. The action of the del operator and Laplacian on this gauge is given by

$$\begin{aligned}\nabla\exp\left(-i\frac{\mathrm{e}}{\hbar}\mathbf{A}_j\cdot\mathbf{r}\right) &= \exp\left(-i\frac{\mathrm{e}}{\hbar}\mathbf{A}_j\cdot\mathbf{r}\right)\left(-i\frac{\mathrm{e}}{\hbar}\mathbf{A}_j + \nabla\right) \\ \Delta\exp\left(-i\frac{\mathrm{e}}{\hbar}\mathbf{A}_j\cdot\mathbf{r}\right) &= \exp\left(-i\frac{\mathrm{e}}{\hbar}\mathbf{A}_j\cdot\mathbf{r}\right)\left(-\frac{\mathrm{e}^2}{\hbar^2}A_j^2 - 2i\frac{\mathrm{e}}{\hbar}\mathbf{A}_j\cdot\nabla + \Delta\right)\end{aligned} \tag{4.125}$$

Combining this result with Eqs. (4.123) and (4.124) yields

$$\begin{aligned}T|\chi_j\rangle = &-\frac{h^2}{8\pi^2 m}\exp\left(-i\frac{\mathrm{e}}{\hbar}\mathbf{A}_j\cdot\mathbf{r}\right) \\ &\times\left[\Delta + 2i\frac{\mathrm{e}}{\hbar}(\mathbf{A}-\mathbf{A}_j)\cdot\nabla - \frac{\mathrm{e}^2}{\hbar^2}(\mathbf{A}-\mathbf{A}_j)\cdot(\mathbf{A}-\mathbf{A}_j)\right]|\phi_j\rangle\end{aligned} \tag{4.126}$$

The first term in the brackets is the usual kinetic energy term, while the second term produces the orbital Zeeman effect. The third term describes the second-order interactions corresponding to the atomic contribution to the susceptibility. The second term can easily be converted into the more familiar form of the Zeeman operator as follows:

$$\begin{aligned}\frac{\mathrm{e}}{m}(\mathbf{A}-\mathbf{A}_j)\cdot\left(\frac{\hbar}{i}\nabla\right) &= \frac{\mathrm{e}}{2m}\mathbf{B}\cdot\big[(\mathbf{r}-\mathbf{R}_j)\wedge\mathbf{p}\big]\\ &= \frac{\mathrm{e}}{2m}\boldsymbol{l}\cdot\mathbf{B}\\ &= -\boldsymbol{m}\cdot\mathbf{B}\end{aligned} \tag{4.127}$$

Here, $\mathbf{p}$ is the momentum operator of the electron in atom j, $\boldsymbol{l}$ is the corresponding angular momentum operator, and $\boldsymbol{m}$ is the magnetic dipole operator. These operators are related by

$$\boldsymbol{m} = -\frac{\mathrm{e}}{2m}\boldsymbol{l} = -\frac{\mu_\mathrm{B}}{\hbar}\boldsymbol{l} \tag{4.128}$$

Here μ_B is the Bohr magneton. Angular momentum is thus expressed in units of $\hbar$, and the magnetic moment in units of the Bohr magneton. The basis atomic orbitals will be eigenfunctions of the first two operators. So to first order the London basis orbitals are eigenfunctions of the total Hamiltonian. Moreover, for a p_z-orbital, the Zeeman effect for a magnetic field along the z-axis vanishes. As a result, the on-site parameter α is independent of the London gauge:

$$\langle\chi_j|\mathcal{H}|\chi_j\rangle = \alpha\langle\chi_j|\chi_j\rangle = \alpha \tag{4.129}$$

However, the inter-site integrals, which depend on the potential energy, V, are influenced by the gauge factors:

$$\langle\chi_i|V|\chi_j\rangle = \left\langle\phi_i\middle|V\exp\left(i\frac{\mathrm{e}}{\hbar}(\mathbf{A}_i-\mathbf{A}_j)\cdot\mathbf{r}\right)\middle|\phi_j\right\rangle \tag{4.130}$$

At this point London introduced an important approximation by replacing the variable position vector in this equation by the position vector (relative to the arbitrary origin) of the center of the bond between the two atoms:

$$\mathbf{r} = (\mathbf{R}_i+\mathbf{R}_j)/2 \tag{4.131}$$

In this approximation the phase factor is turned into a constant, which can be removed from the brackets. One has:

$$\begin{aligned}\frac{1}{2}(\mathbf{A}_i-\mathbf{A}_j)\cdot(\mathbf{R}_i+\mathbf{R}_j) &= \frac{1}{4}\big[(\mathbf{B}\wedge\mathbf{R}_i)\cdot\mathbf{R}_j-(\mathbf{B}\wedge\mathbf{R}_j)\cdot\mathbf{R}_i\big]\\ &= \frac{1}{2}\mathbf{B}\cdot(\mathbf{R}_i\wedge\mathbf{R}_j)\\ &= \mathbf{B}\cdot\mathbf{S}_{ij}\end{aligned} \tag{4.132}$$

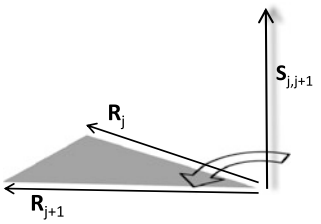

Fig. 4.8 Triangular surface vector: $\mathbf{S}_{j,j+1} = \frac{1}{2}\mathbf{R}_j \wedge \mathbf{R}_{j+1}$

Here $\mathbf{S}_{ij}$ is the directed area of the triangle formed by the position vectors of the atoms i and j from the origin, as shown in Fig. 4.8. The orientation of the vector $\mathbf{S}_{ij}$ follows the right thumb rule. So if the atom numbers increase counterclockwise, this vector will be oriented in the positive z-direction. One also has:

$$\mathbf{S}_{ij} = -\mathbf{S}_{ji} \tag{4.133}$$

The interaction elements in the Hückel matrix are thus replaced by

$$\begin{aligned} \langle \chi_i | V | \chi_j \rangle &= \exp\left(i \frac{\mathrm{e}}{\hbar} \mathbf{B} \cdot \mathbf{S}_{ij} \right) \beta \\ \langle \chi_j | V | \chi_i \rangle &= \exp\left(-i \frac{\mathrm{e}}{\hbar} \mathbf{B} \cdot \mathbf{S}_{ij} \right) \beta \end{aligned} \tag{4.134}$$

We further define a vector $\mathbf{S}$ as

$$\sum_{j=0}^{N-1} \mathbf{S}_{j,j+1} = \mathbf{S} \tag{4.135}$$

The magnitude of this vector is equal to the area of the polygon. Because of cyclic symmetry, we can also write

$$\mathbf{S}_{j,j+1} = \frac{1}{N} \mathbf{S} \tag{4.136}$$

The action of the symmetry operators on the London gauge is as follows:

$$\begin{aligned} \hat{C}_N \exp\left(-i \frac{\mathrm{e}}{\hbar} \mathbf{A}_j \cdot \mathbf{r} \right) &= \exp\left[-i \frac{\mathrm{e}}{\hbar} \mathbf{A}_j \cdot \left(\hat{C}_N^{-1} \mathbf{r} \right) \right] \\ &= \exp\left(-i \frac{\mathrm{e}}{\hbar} \mathbf{A}_{j+1} \cdot \mathbf{r} \right) \end{aligned} \tag{4.137}$$

which may easily be proven by writing out $\mathbf{A}_j$ and $\hat{C}_N^{-1}\mathbf{r}$ in full. Hence, the rotation axis will perform a cyclic permutation of the $|\chi_j\rangle$ kets, exactly in the same way as for the $|\phi_j\rangle$ kets. The magnetic field reduces the D_{nh} symmetry of the regular polygon to C_{nh} (see Appendix B), so the cyclic symmetry is conserved, and thus the projection operators of Eq. (4.114) remain valid, and so do the eigenfunctions.

We shall denote these as $|\Psi_k\rangle$. One has:

$$|\Psi_k\rangle = \frac{1}{\sqrt{N}} \sum_{j=0}^{N-1} \exp\left(2\pi i \frac{jk}{N}\right) |\chi_j\rangle \tag{4.138}$$

The corresponding eigenvalues can be worked out in the same way as in the absence of the field (see Eq. (4.119)):

$$\begin{aligned} E_k &= \langle \Psi_k | \mathcal{H} | \Psi_k \rangle \\ &= \frac{1}{N} \sum_{j,j'=0}^{N-1} \exp\left(2\pi i \frac{k(-j+j')}{N}\right) \langle \chi_j | \mathcal{H} | \chi_{j'} \rangle \\ &= \alpha + \frac{1}{N} \sum_{j=0}^{N-1} \beta \left[\exp\left(-\frac{2\pi i k}{N} + i \frac{\mathrm{e}}{\hbar} \mathbf{B} \cdot \mathbf{S}_{j,j-1}\right) + \exp\left(\frac{2\pi i k}{N} + i \frac{\mathrm{e}}{\hbar} \mathbf{B} \cdot \mathbf{S}_{j,j+1}\right) \right] \\ &= \alpha + 2\beta \cos\left[\frac{2\pi}{N} \left(k + \frac{\mathrm{e}}{\hbar} \mathbf{B} \cdot \mathbf{S} \right) \right] \end{aligned} \tag{4.139}$$

The result is of the same form as in the absence of the field, except for a shift of the quantum number k under the influence of the magnetic field. The magnitude of this shift, $\mathrm{e}/\hbar \mathbf{B} \cdot \mathbf{S}$, is equal to the magnetic flux through the area of the ring, multiplied by the constant $\mathrm{e}/\hbar$. As a result of this shift, the energy levels that were originally degenerate now display a Zeeman splitting. For $\mathbf{B} \cdot \mathbf{S} > 0$, the Zeeman contribution adds to k in the energy expression. This implies that the points on the k axis in Fig. 4.7 are displaced to the right. The roots with $k = 1, 2$ thus increase in energy, while their counterparts, $k = -1, -2$, become lower in energy. Likewise, the root at the bottom ($k = 0$) increases in energy, while the root at the top, $k = 3$, decreases, but the changes in these extremal points are only of second order.

This simple model is at the basis of a whole corpus of electromagnetic studies of conjugated polyenes, involving, inter alia, the calculation of magnetic susceptibilities, current densities, ring currents, and chemical shifts in nuclear magnetic resonance (NMR). From the point of view of symmetry, it is to be noted that the magnetic field has removed all degeneracies. The time-reversal symmetry is indeed no longer valid. However, if one reverses the momenta, $k \to -k$, and at the same time switches the magnetic field, $\mathbf{B} \to -\mathbf{B}$, the energies are still invariant. This operation is no longer an invariance operation of one measurement though, but rather a comparison between two separate experiments with opposite fields.

Polyhedral Hückel Systems of Equivalent Atoms

The polygonal system of the annulenes can be extended to polyhedral systems of equivalent atoms. Atoms are equivalent if the symmetry group of the molecule—or

more generally the automorphism group of the molecular graph—acts transitively on the set of atomic nodes. So, for any pair of atoms $\langle k\rangle\langle l\rangle$, there is a symmetry element that will map $\langle k\rangle$ onto $\langle l\rangle$, and then of course there is always an inverse element that maps $\langle l\rangle$ onto $\langle k\rangle$. The solution of the Hamiltonian matrix for such a system can almost entirely be performed by symmetry arguments. The first step consists in the construction of SALCs, using the projection operators on the atomic orbital on site $\langle a\rangle$:

$$|\Phi_{ik}^{\Omega}\rangle = \hat{P}_{ik}^{\Omega}|\phi_{\mathrm{A}}\rangle = \frac{\dim(\Omega)}{|G|}\sum_{R\in G}\bar{D}_{ik}^{\Omega}(R)\hat{R}|\phi_{\mathrm{A}}\rangle \tag{4.140}$$

These functions are not yet normalized. This can be done later. Let us first consider a general matrix element:

$$\begin{aligned}\left\langle\Phi_{ik}^{\Omega}|\mathcal{H}|\Phi_{jl}^{\Omega'}\right\rangle &= \frac{\dim(\Omega)^2}{|G|^2}\sum_{R,S}D_{ik}^{\Omega}(R)\bar{D}_{jl}^{\Omega'}(S)\langle\hat{R}\phi_{\mathrm{A}}|\mathcal{H}|\hat{S}\phi_{\mathrm{A}}\rangle\\ &= \frac{\dim(\Omega)^2}{|G|^2}\sum_{R,Q}D_{ik}^{\Omega}(R)\bar{D}_{jl}^{\Omega'}(RQ)\langle\hat{R}\phi_{\mathrm{A}}|\mathcal{H}|\hat{RQ}\phi_{\mathrm{A}}\rangle\\ &= \frac{\dim(\Omega)^2}{|G|^2}\sum_{R,Q}\sum_{m}D_{ik}^{\Omega}(R)\bar{D}_{jm}^{\Omega'}(R)\bar{D}_{ml}^{\Omega'}(Q)\left\langle\phi_{\mathrm{A}}|\hat{R}^{-1}\mathcal{H}\hat{R}|\hat{Q}\phi_{\mathrm{A}}\right\rangle\\ &= \frac{\dim(\Omega)}{|G|}\delta_{\Omega\Omega'}\delta_{ij}\sum_{Q}\bar{D}_{kl}^{\Omega}(Q)\langle\phi_{\mathrm{A}}|\mathcal{H}|\hat{Q}\phi_{\mathrm{A}}\rangle\end{aligned} \tag{4.141}$$

The by-now experienced reader has recognized in the second line of this derivation the use of a substitution, $\hat{S}\to\hat{R}\hat{Q}$, as well as the invariance of the Hamiltonian under the symmetry transformation in the third line. Let us now use this equation to normalize the SALCs. This can be done by simply setting the Hamiltonian equal to unity. Adopting the Hückel approximation, which neglects all overlaps between the sites, we obtain:

$$\left\langle\Phi_{ik}^{\Omega}|\Phi_{ik}^{\Omega}\right\rangle = \frac{\dim(\Omega)}{|G|}\sum_{Q}\bar{D}_{kk}^{\Omega}(Q)\delta_{Q,E} = \frac{\dim(\Omega)}{|G|} \tag{4.142}$$

Hence, the normalized SALCs should be redefined as

$$|\Phi_{ik}^{\Omega}\rangle = \sqrt{\frac{\dim(\Omega)}{|G|}}\sum_{R\in G}\bar{D}_{ik}^{\Omega}(R)\hat{R}|\phi_{\mathrm{A}}\rangle \tag{4.143}$$

The matrix elements are accordingly simplified to

$$\left\langle\Phi_{ik}^{\Omega}|\mathcal{H}|\Phi_{il}^{\Omega}\right\rangle = \sum_{Q}\bar{D}_{kl}^{\Omega}(Q)\langle\phi_{\mathrm{A}}|\mathcal{H}|\hat{Q}\phi_{\mathrm{A}}\rangle \tag{4.144}$$

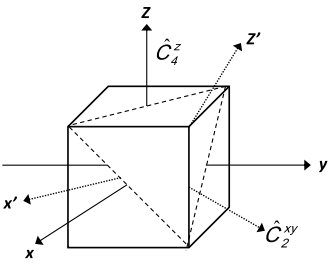

Fig. 4.9 Orientation in a cube of a tetragonal (x, y, z) and trigonal (x', y', z') system. The symmetry elements $\hat{C}_4^z$, $(\hat{C}_4^z)^{-1}$, and $\hat{C}_2^{xy}$ take the trigonal site to its nearest neighbors

The Hückel approximation considers only hopping between nearest neighbors, and hence the sum in this expression is limited to only those operators that link the starting site to its neighbours. We thus do not need all the irrep matrices, but only a few of them. As an example, the cube is a trivalent polyhedron, i.e., each atom has three bonds to its neighbors. The neighbors of site $\langle a \rangle$ can be reached by $\hat{C}_4, \hat{C}_4^{-1}, \hat{C}_2^{xy}$, where the twofold axis belongs to the $6\hat{C}_2'$ class. We thus need to know the irrep matrices for these three elements only. In principle, according to the above derivation, for each component of each irrep, we can, by varying the index k, construct a number of projection operations which is equal to $\dim(\Omega)$. As we have already discussed, we effectively need all these only when the induced representation of the atoms is equal to the regular representation. This is the case if the number of atoms is equal to the order of the group, i.e., when there are no symmetry elements "going through" the atoms, so that their site group is the trivial C_1. For octahedral symmetry, this is a polyhedron with 48 vertices. It belongs to the family of the Archimedean solids and is known as the *great rhombicuboctahedron*. The highest Archimedean solid is a polyhedron with 120 equivalent vertices, which is known as the *great rhombicosidodecahedron*.[3] The representation of its vertices is the regular representation of the group I_h. In the case where the number of atoms is less, and thus the site symmetry is higher, the projection operators will give rise to redundancies. To avoid these, we can make use of the Frobenius reciprocity theorem. The number of times a given irrep occurs in the induction is exactly equal to the number of times it subduces the totally symmetric irrep at the site group. The number of projection operations should thus also be restricted to this number. This can be achieved when the $\mathbb{D}^{\Omega}$ matrices are constructed in such a way that they are block diagonal in the stabilizing sitegroup of site $\langle a \rangle$. In that case the k indices of the projection operators should then be chosen in such a way that they correspond to components that are totally symmetric in that sitegroup.[4] As an example, consider the cube. The site group is C_{3v}, and induction tells us that the function space, spanned by the 8 atoms, is given by

$$\Gamma(a_1 C_{3v} \uparrow Oh) = A_{1g} + T_{2g} + T_{1u} + A_{2u} \tag{4.145}$$

[3] Calculations predict that a C_{120} molecular realization of this solid should exist. See [11, 12].

[4] For more elaborate treatments, including the use of the Cayley graph, see [13, 14].

All these irreps occur only once; hence, when we choose a trigonal symmetry adaptation for constructing representation matrices, for all these matrices, there will be exactly one index k that labels the component that is totally symmetric in C_{3v}. For this value, the matrix elements read

$$\langle \Phi_{ik}^{\Omega} | \mathcal{H} | \Phi_{ik}^{\Omega} \rangle = \beta \big[\bar{D}_{kk}^{\Omega}(C_4) + \bar{D}_{kk}^{\Omega}\big(C_4^{-1}\big) + \bar{D}_{kk}^{\Omega}(C_2) \big] \tag{4.146}$$

To obtain these eigenvalues, we thus have to mould the representation matrices for O_h in a trigonal setting. For the one-dimensional irreps, A_{1g} and A_{2u}, this is trivial since the matrix elements in Eq. (4.146) are simply the characters. We thus obtain:

$$\begin{aligned} E(A_{1g}) &= \beta \big[\chi^{A_{1g}}(C_4) + \chi^{A_{1g}}\big(C_4^{-1}\big) + \chi^{A_{1g}}(C_2) \big] = 3\beta \\ E(A_{2u}) &= \beta \big[\chi^{A_{2u}}(C_4) + \chi^{A_{2u}}\big(C_4^{-1}\big) + \chi^{A_{2u}}(C_2) \big] = -3\beta \end{aligned} \tag{4.147}$$

For the T_{1u} irrep, we can use the set of the p-orbitals. In the standard Cartesian orientation, this set is adapted to the tetragonal site symmetry. In Fig. 4.9 we illustrate an alternative trigonal basis (see also Fig. 3.6(d)). The transformation between the two sets is given by

$$\begin{aligned} |p_z'\rangle &= \frac{1}{\sqrt{3}} \big(|p_x\rangle + |p_y\rangle + |p_z\rangle \big) \\ |p_x'\rangle &= \frac{1}{\sqrt{2}} \big(|p_x\rangle - |p_y\rangle \big) \\ |p_y'\rangle &= \frac{1}{\sqrt{6}} \big(|p_x\rangle + |p_y\rangle - 2|p_z\rangle \big) \end{aligned} \tag{4.148}$$

Here, the first component points in the threefold direction and thus is adapted to the C_{3v} site symmetry. We require only the diagonal matrix elements for this component. They can easily be obtained by expressing these elements in the standard canonical set:

$$\begin{aligned} D_{z'z'}(C_4) &= \langle p_z' | \hat{C}_4 | p_z' \rangle \\ &= \frac{1}{3} \big(\langle p_x | + \langle p_y | + \langle p_z | \big) \hat{C}_4 \big(|p_x\rangle + |p_y\rangle + |p_z\rangle \big) \\ &= \frac{1}{3} \big(\langle p_x | + \langle p_y | + \langle p_z | \big) \big(|p_y\rangle - |p_x\rangle + |p_z\rangle \big) = \frac{1}{3} \\ D_{z'z'}\big(C_4^{-1}\big) &= \langle p_z' | \hat{C}_4^{-1} | p_z' \rangle \\ &= \frac{1}{3} \big(\langle p_x | + \langle p_y | + \langle p_z | \big) \hat{C}_4^{-1} \big(|p_x\rangle + |p_y\rangle + |p_z\rangle \big) \\ &= \frac{1}{3} \big(\langle p_x | + \langle p_y | + \langle p_z | \big) \big(-|p_y\rangle + |p_x\rangle + |p_z\rangle \big) = \frac{1}{3} \end{aligned}$$

$$
\begin{aligned}
D_{z'z'}(C_2') &= \langle p_z'|\hat{C}_2'|p_z'\rangle \\
&= \frac{1}{3}\big(\langle p_x| + \langle p_y| + \langle p_z|\big)\hat{C}_2'\big(|p_x\rangle + |p_y\rangle + |p_z\rangle\big) \\
&= \frac{1}{3}\big(\langle p_x| + \langle p_y| + \langle p_z|\big)\big(|p_y\rangle + |p_x\rangle - |p_z\rangle\big) = \frac{1}{3}
\end{aligned}
\tag{4.149}
$$

An entirely similar derivation can be made for the T_{2g} irrep, using the d-orbital set. The results are:

$$
\begin{aligned}
E(T_{1u}) &= \beta \\
E(T_{2g}) &= -\beta
\end{aligned}
\tag{4.150}
$$

Triphenylmethyl Radical and Hidden Symmetry

As a final application, we discuss an example of a molecular radical, where more symmetry is present than the eye meets. The triphenylmethyl radical, $C_{19}H_{15}$, is a planar, conjugated, hydrocarbon-radical, with 19 π-electrons. The molecular point group for the planar configuration is D_{3h}, but, since all valence $2p_z$-orbitals are antisymmetric with respect to the horizontal symmetry plane, the relevant symmetry of the valence shell is only C_{3v} as seen from Fig. 4.10. The molecular symmetry group distributes the 19 atoms over five trigonal orbits of atoms that, under C_{3v}, can solely be permuted with partners in the same orbit.

1. The central atom {o}.
2. The three atoms that are adjacent to o: $\{a, b, c\}$.
3. The six atoms in the *ortho* positions: $\{d, e, f, g, h, i\}$.
4. The six atoms in the *meta* positions: $\{p, q, r, s, t, u\}$.
5. The three atoms in the *para* positions: $\{x, y, z\}$.

The separate rotation of a single phenyl group by 180° around its twofold direction will not change the connectivity of the graph. Yet this cannot be achieved by elements of the point group. It is, however, a legitimate symmetry operation as far as the graph is concerned since it preserves the connectivity. The resulting automorphism group is thus larger than the point group and in fact is isomorphic to O_h [15]. The three phenyl groups can be associated with the three Cartesian directions of this octahedral group. The six atoms in the ortho orbit can be formally associated with the six corners of this octahedron, each connected to a meta position (Fig. 4.10). This implies that the ortho and meta atoms occupy C_{4v} sites. The three-atom orbits correspond to the three tetragonal directions in the octahedron. The site group that leaves such a tetragonal direction invariant is not of the conical C_{nv} type, but D_{4h}. These correspondences allow identification of all the permutations. As examples, the $\hat{C}_4$ symmetry element through the upper phenyl group and the $\hat{S}_6$ rotation–reflection

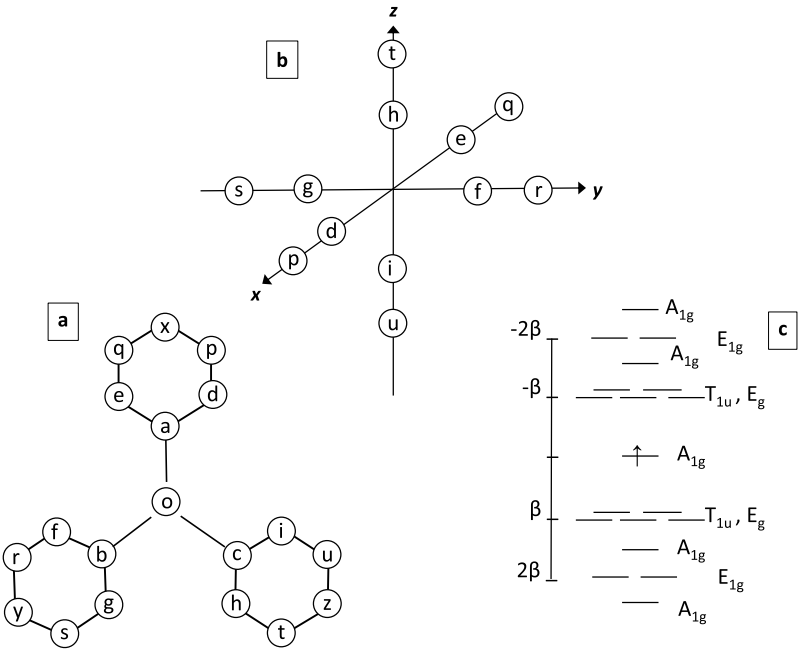

Fig. 4.10 (**a**) molecular graph of triphenylmethyl, (**b**) correspondence between ortho and meta sites and octahedral C_{4v} positions, and (**c**) Hückel spectrum

extension along the threefold direction of the trigonal axis of the molecular frame permute the atoms as follows:

$$\begin{aligned}\hat{C}_4 &\to (o)(a)(d)(p)(x)(q)(e)(b,c)(y,z)(f,h,g,i)(r,t,s,u)\\ \hat{S}_6 &\to (o)(a,c,b)(x,z,y)(d,i,f,e,h,g)(p,u,r,q,t,s)\end{aligned} \tag{4.151}$$

A horizontal coordinate plane, $\hat{\sigma}_h$, of the octahedron has the effect of flipping one single phenyl group around. We can at once determine the irreps of the different orbits by induction:

$$\begin{aligned}\{a,b,c\} &: \Gamma(a_{1g}D_{4h} \uparrow O_h) = A_{1g} + E_g\\ \{x,y,z\} &: \Gamma(a_{1g}D_{4h} \uparrow O_h) = A_{1g} + E_g\\ \{d,e,f,g,h,i\} &: \Gamma(a_1C_{4v} \uparrow O_h) = A_{1g} + E_g + T_{1u}\\ \{p,q,r,s,t,u\} &: \Gamma(a_1C_{4v} \uparrow O_h) = A_{1g} + E_g + T_{1u}\end{aligned} \tag{4.152}$$

The central atom is invariant in O_h and thus transforms as A_{1g}. The total induced representation of the function space thus is given by

$$\Gamma = 5A_{1g} + 4E_g + 2T_{1u} \tag{4.153}$$

The 19-dimensional Hückel matrix thus will be resolved into five blocks, one of dimension 5, two identical blocks of dimension 4, and three identical blocks of dimension 2. In Table 4.9 we display the blocks for each irrep and the corresponding SALCs for one component. The corresponding secular equations are:

$$\begin{aligned} A_{1g} &: \lambda\left(\lambda^4 - 8\lambda^2 + 13\right)^2 = 0 \\ E_g &: \lambda^4 - 5\lambda^2 + 4 = 0 \\ T_{1u} &: \lambda^2 - 1 = 0 \end{aligned} \tag{4.154}$$

Symmetry has taken us to a point where still quintic, quartic, and quadratic secular equations must be solved. However, a closer look at this equations shows that they can easily be solved. Apparently, a further symmetry principle is present, which leads to simple analytical solutions of the secular equations. Triphenylmethyl is an *alternant* hydrocarbon. In an alternant, atoms can be given two different colors in such a way that all bonds are between atoms of different colors; hence, no atoms of the same color are adjacent. A graph with this property is *bipartite*,[5] and its eigenvalue spectrum obeys the celebrated Coulson–Rushbrooke theorem [16].

Theorem 8 *The eigenvalues of an alternant are symmetrically distributed about the zero energy level. The corresponding eigenfunctions also show a mirror relationship, except for a difference of sign* (*only*) *in every other atomic orbital coefficient. The total charge density at any carbon atom in the neutral alternant hydrocarbon equals unity.*

Since triphenylmethyl is an odd alternant, there should be at least one eigenvalue at energy zero. This root will be necessarily of A_{1g} symmetry since this is the only irrep that occurs an odd number of times. All other roots occur in pairs of opposite energies. This is confirmed by the secular equations in Eq. (4.154), where the A_{1g} equation indeed has a root at $\lambda = 0$, and all remaining equations contain only even powers of λ. The roots are then easily determined (see also Fig. 4.10):

$$\begin{aligned} A_{1g} &: \lambda = 0, \pm\sqrt{4 \pm \sqrt{3}} \\ E_g &: \lambda = \pm 1, \pm 2 \\ T_{1u} &: \lambda = \pm 1 \end{aligned} \tag{4.155}$$

[5] Note that in fact a molecular graph will always be bipartite unless it contains one or more odd-membered rings.

Table 4.9 SALCs and Hückel matrices, in units of β, for triphenylmethyl. For the degenerate irreps, only one component is given

$\mathbf{A}_{1g}$					
$\|o\rangle$	$-\lambda$	$\sqrt{3}$	0	0	0
$1/\sqrt{3}(\|a\rangle + \|b\rangle + \|c\rangle)$	$\sqrt{3}$	$-\lambda$	0	$\sqrt{2}$	0
$1/\sqrt{3}(\|x\rangle + \|y\rangle + \|z\rangle)$	0	0	$-\lambda$	0	$\sqrt{2}$
$1/\sqrt{6}(\|d\rangle + \|e\rangle + \|f\rangle + \|g\rangle + \|h\rangle + \|i\rangle)$	0	$\sqrt{2}$	0	$-\lambda$	1
$1/\sqrt{6}(\|p\rangle + \|q\rangle + \|r\rangle + \|s\rangle + \|t\rangle + \|u\rangle)$	0	0	$\sqrt{2}$	1	$-\lambda$
$\mathbf{E}_g$					
$1/\sqrt{2}(\|b\rangle - \|c\rangle)$		$-\lambda$	0	$\sqrt{2}$	0
$1/\sqrt{2}(\|y\rangle - \|z\rangle)$		0	$-\lambda$	0	$\sqrt{2}$
$1/2(\|f\rangle + \|g\rangle - \|h\rangle - \|i\rangle)$		$\sqrt{2}$	0	$-\lambda$	1
$1/2(\|r\rangle + \|s\rangle - \|t\rangle - \|u\rangle)$		0	$\sqrt{2}$	1	$-\lambda$
$\mathbf{T}_{1u}$					
$1/\sqrt{2}(\|d\rangle - \|e\rangle)$				$-\lambda$	1
$1/\sqrt{2}(\|p\rangle - \|q\rangle)$				1	$-\lambda$

The spectrum contains unexpected fivefold degeneracies at $E = \pm\beta$, where the T_{1u} and E_g levels coincide. This degeneracy is considered *accidental*, to the extent that it does not correspond to a single irrep of the automorphism group of the graph. However, the fivefold degeneracy can easily be rationalized as follows: $E = \beta$ is the eigenenergy of the degenerate highest occupied molecular orbital (HOMO) in an isolated phenyl-ring. The three rings thus give rise to six orbitals with this energy. The symmetry of this orbital space in O_h is equal to $A_{1g} + E_g + T_{1u}$. Of these only the A_{1g} combination is of the right symmetry to interact with the central atom. For the five others, there can be no communication between the phenyl rings since the channel via the central atom is open only to A_{1g} symmetries. As a result, for these solutions, there is no overlap between the rings, and five isolated phenyl solutions persist at $E = \beta$. A similar argument applies to the level $E = -\beta$, which stems from the phenyl lowest unoccupied orbital (LUMO).

Many features thus come together in triphenylmethyl. Besides the C_{3v} molecular point group, the Hückel matrix obeys an additional or hidden O_h symmetry. This is a typical feature of the nearest-neighbor approximation, which requires only that symmetry operations should preserve the connections with the nearest neighbors. This precisely complies with the definition of the automorphism group of the graph. Furthermore, the special bipartite properties of the graph further impose constraints on the spectrum, which in this case lead to a complete reduction of the secular equations. Finally, an unexpected additional degeneracy manifests itself, which is related

to the composite nature of the molecule being considered, with several fragments bound to one central atom.

4.10 Problems

4.1 A Schlegel diagram of a polyhedron is a projection into a plane figure. The figure below shows the Schlegel diagram for a dodecahedron. As was explained in the preceding chapter (see Fig. 3.8(a)), a dodecahedron contains five cubes, e.g., the cube based on the nodes $\langle 1, 3, 9, 10, a, c, i, j \rangle$. Symmetry elements of I_h permute these cubes. Construct the set of the five cubes and determine the irreps of this set. Can you obtain this result by induction?

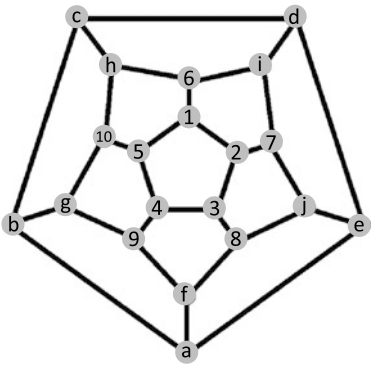

4.2 Consider the set of eight tangential π-orbitals on a tetrahedron. Derive the irreducible representations in the T_d point group. How would you label the canonical symmetry of the combinations that are shown in the figure below?

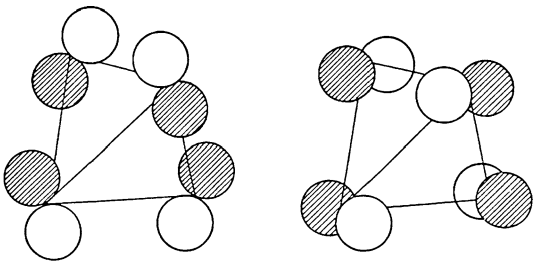

4.3 Consider the set of perpendicular p_z-orbitals in the polyaromatic planar molecule coronene shown below. This set gives rise to a symmetry of molecular orbitals of a_{1u} and b_{1g} . Can you draw both these orbitals? (Use the standard orientation of the central benzene frame, as shown in Fig. 3.10)

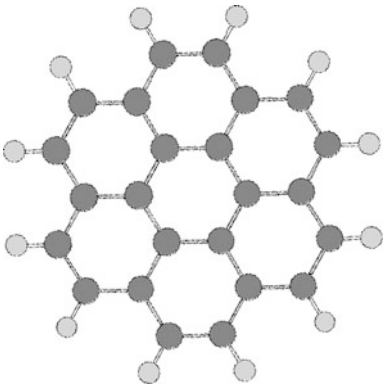

4.4 In dodecaborane, $B_{12}H_{12}^{2-}$, the twelve boron atoms occupy the vertices of an icosahedral cage. Determine the irreducible representations of the set of their tangential π-orbitals.

4.5 Consider a degenerate manifold, transforming as the irrep Γ_i. The appropriate projector was applied to the basis to yield one component of the degeneracy space. Which other projectors do you need to use to generate all the remaining components?

4.6 Consider the expression for a totally symmetric projection operator and demonstrate that it is indeed totally symmetric under any group element.

4.7 Construct the three sp^2 hybrids in the xy plane.

4.8 The picture below shows the distortion of an equilateral triangle. Determine the representation of this distortion.

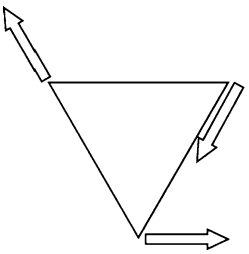

4.9 Construct the character table for a cyclic group of order 5.

4.10 In a molecule with D_{6h} symmetry, the choice of $\hat{C}_2'$ and $\hat{C}_2''$ directions is arbitrary, but, once the twofold directions are chosen, the $\hat{\sigma}_v$ and $\hat{\sigma}_d$ reflection planes are also fixed, as was indicated in Fig. 3.10. Show that these spatial relationships between the axes and the planes is in line with the character table for D_{6h}.

4.11 Consider a molecule with D_{3h} symmetry and apply a distortion mode that transforms according to the a_2'' irrep. A distortion along this coordinate breaks

the original symmetry to a subgroup of D_{3h}. Which subgroup? Try to generalize this example to a general rule.

4.12 Below is shown the Schlegel diagram for the C_{24} fullerene. It is a cage structure with hexagonal faces at top and bottom, capping a crown of twelve pentagons around its waist. The valence shell of this structure is formed by a set of 24 radial p_σ-orbitals, one on each carbon. Determine the point group of this molecule and the irreps describing the valence shell. (Hint: divide the set of 24 orbitals into two separate orbits.)

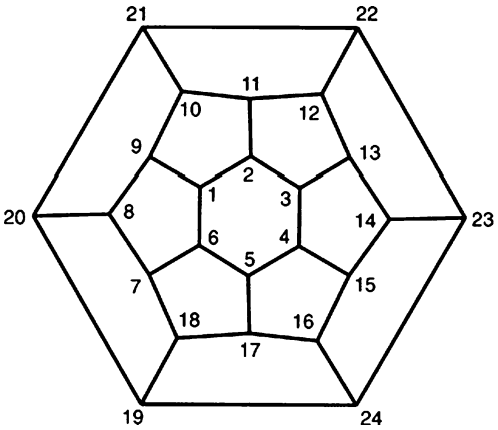

References

1. Mulliken, R.S.: Report on notation for the spectra of polyatomic molecules. J. Chem. Phys. **23**, 1997 (1955)
2. Altmann, S.L.: Induced Representations in Crystals and Molecules. Academic Press, London (1977)
3. Ceulemans, A.: The construction of symmetric orbitals for molecular clusters. Mol. Phys. **54**, 161 (1985)
4. Shimanouchi, T.: Tables of Molecular Vibrational Frequencies Consolidated, Vol. I. National Bureau of Standards, Gaithersburg, Maryland (1972)
5. Yun-Guang, Z., Yu-De, L.: Relativistic density functional investigation of UX_6 (X=F, Cl, Br and I). Chin. Phys. **19**, 033302 (2010)
6. Aldridge, J.P., et al.: Measurement and analysis of the infrared-active stretching fundamental (ν_3) of UF_6. J. Chem. Phys. **83**, 34 (1985)
7. Salem, L.: The Molecular Orbital Theory of Conjugated Systems. W. A. Benjamin, New York and Amsterdam (1966)
8. Coulson, C.A., O'Leary, B., Mallion, R.B.: Hückel Theory for the Organic Chemists. Academic Press, London (1978)
9. Cvetković, D.M., Doob, M., Sachs, H.: Spectra of Graphs, 3rd edn. Johann Ambrosius Barth Verlag, Heidelberg (1995)

10. London, F.: Théorie quantique des courants interatomiques dans les combinaisons aromatiques. J. Phys. Radium **8**, 397 (1937)
11. Schulman, J.M., Dish, R.L.: Archimedene. Chem. Phys. Lett. **262**, 813 (1996)
12. Bruns, D., Miura, H., Vollhardt, K.P., Stanger, A.: En route to archimedene: total synthesis of C_{3h}-symmetric [7]phenylene. Org. Lett. **5**, 549 (2003)
13. Fowler, P.W., Ceulemans, A., Chibotaru, L.F.: Eigenvalues of Hückel systems of equivalent points. Discrete Math. **212**, 75 (2000)
14. Samuel, S.: On the electronic structure of C_{60}. Int. J. Mod. Phys. B **7**, 3877 (1993)
15. Ojha, P.C.: Analysis of degeneracy in the spectrum of a class of molecular graphs. Int. J. Quant. Chem. **35**, 687 (1989)
16. Mallion, R.B., Rouvray, D.H.: The golden jubilee of the Coulson–Rushbrooke pairing theorem. J. Math. Chem. **5**(1), 399 (1990). See also J. Math. Chem. 8, 1991